Published in final edited form as:
Development. 2004 May ; 131(9): 2205–2218. doi:10.1242/dev.01086.

BMP receptor IA is required in mammalian neural crest cells for development of the cardiac outflow tract and ventricular myocardium

Rolf W. Stottmann[1], **Murim Choi**[1], **Yuji Mishina**[2], **Erik N. Meyers**[1,3], and **John Klingensmith**[1,*]

[1]Department of Cell Biology, Duke University Medical Center, Durham, NC 27710, USA

[2]Laboratory of Reproductive and Developmental Toxicology, National Institute of Environmental Health Sciences, Research Triangle Park, NC 27709, USA

[3]Department of Pediatrics, Duke University Medical Center, Durham, NC 27710, USA

Summary

The neural crest is a multipotent, migratory cell population arising from the border of the neural and surface ectoderm. In mouse, the initial migratory neural crest cells occur at the five-somite stage. Bone morphogenetic proteins (BMPs), particularly BMP2 and BMP4, have been implicated as regulators of neural crest cell induction, maintenance, migration, differentiation and survival. Mouse has three known BMP2/4 type I receptors, of which *Bmpr1a* is expressed in the neural tube sufficiently early to be involved in neural crest development from the outset; however, earlier roles in other domains obscure its requirement in the neural crest. We have ablated *Bmpr1a* specifically in the neural crest, beginning at the five-somite stage. We find that most aspects of neural crest development occur normally; suggesting that BMPRIA is unnecessary for many aspects of early neural crest biology. However, mutant embryos display a shortened cardiac outflow tract with defective septation, a process known to require neural crest cells and to be essential for perinatal viability. Surprisingly, these embryos die in mid-gestation from acute heart failure, with reduced proliferation of ventricular myocardium. The myocardial defect may involve reduced BMP signaling in a novel, minor population of neural crest derivatives in the epicardium, a known source of ventricular myocardial proliferation signals. These results demonstrate that BMP2/4 signaling in mammalian neural crest derivatives is essential for outflow tract development and may regulate a crucial proliferation signal for the ventricular myocardium.

Keywords

BMPRIA; Neural crest; Heart; Outflow tract; Myocardium; Epicardium

Introduction

The neural crest is a transient vertebrate tissue with a wide variety of cell fates, including peripheral nervous system neurons and glia, melanocytes, smooth muscle cells and most craniofacial cartilages and bones (Le Douarin and Kalcheim, 1999). The neural crest also contributes crucial cell populations to several thoracic tissues, including the developing outflow tract of the heart (Kirby and Waldo, 1995). Neural crest cells (NCCs) delaminate

*Author for correspondence (kling@cellbio.duke.edu).

from the dorsal neural folds, undergo an epithelial to mesenchymal transition, and migrate to target tissues. In mouse, this process starts in the rostral hindbrain around the five somite (5 s) stage (Nichols, 1981), extends to the midbrain, forebrain and caudal hindbrain, and progresses to increasingly caudal trunk levels. At any given axial level, the process of NCC production lasts about 9 hours (Serbedzija et al., 1992). Thus, the early phases of NCC development are ongoing at all axial levels in mouse; for example, in the rostral hindbrain, emigration appears to be complete around 11 s, while it lasts until 14 s in midbrain and caudal hindbrain, and extends to yet later stages at other axial levels (Serbedzija et al., 1992).

In conjunction with several other developmental signaling molecules, bone morphogenetic proteins (BMPs), particularly BMP2 and BMP4, have been implicated in promoting NCC induction, maintenance, migration and differentiation in several different model organisms (Aybar and Mayor, 2002; Christiansen et al., 2000; Knecht and Bronner-Fraser, 2002). Most evidence has come from gain-of-function manipulations, such as application of recombinant BMP proteins, or overexpression of transgenes that modulate BMP signaling. However, zebrafish embryos with reduced BMP2 show deficient NCCs (Nguyen et al., 1998). Mouse embryos null for BMP2 show no evidence of migratory NCCs, but die while neural crest is forming, obscuring the requirement for BMP2 in this process (Kanzler et al., 2000). The involvement of other BMPs and signaling pathway components are masked by earlier roles or, possibly, by functional redundancy. Thus, the requirements for BMP activity in various aspects of mammalian neural crest development remain unclear.

We have used a conditional gene ablation approach to address the requirements for BMP signaling in mammalian NCC biology. BMP ligands activate a bipartite receptor complex composed of a type I and type II receptor (Kawabata et al., 1998). Mouse has three known type I receptors for BMP2 and BMP4, BMPRIA (ALK3), BMPRIB (ALK6) and possibly ActRIA (ALK2) (Miyazono et al., 2001). Neither *Bmpr1b* nor *Actr1a* is expressed in the neural tube until well after NCC migration has begun (Gu et al., 1999; Panchision et al., 2001; Yoshikawa et al., 2000). By contrast, *Bmpr1a* is expressed throughout the early embryo, including the dorsal neural folds, but null mutants fail to gastrulate (Mishina et al., 1995). Fortunately, a conditional null allele of *Bmpr1a* allows the deletion of this gene in tissues expressing Cre recombinase (Mishina et al., 2002). We used a *Wnt1-Cre* transgene, which triggers recombination exclusively in forming NCCs (Brault et al., 2001; Chai et al., 2000; Danielian et al., 1998; Jiang et al., 2000), to delete *Bmpr1a* specifically in the neural crest from the outset of migration. Embryos lacking *Bmpr1a* in NCCs die abruptly at midgestation with no defects in the induction, maintenance, delamination or initial migration of NCCs. Instead, we observed severe defects in the cardiac outflow tract and ventricular myocardium.

Materials and methods

Mouse maintenance and genotyping

Embryos were generated by mating *Wnt1-Cre*/+;*Bmpr1a*^{null}/+ mice with mice homozygous for the *Bmpr1a*^{flox} allele or doubly homozygous for the R26R reporter and the *Bmpr1a*^{flox} allele. All *Bmpr1a* alleles and their genotyping are as published (Mishina et al., 2002). Mutant embryos were identified by PCR genotyping for presence of the Cre transgene (Cre1, TGATGAGGTTCGCAAGAACC; Cre 2, CCATGAGTGAACGAACCTGG) and a null allele of *Bmpr1a*. R26R alleles were identified by a 250 bp PCR product (R26R-1, AAAGTCGCTCTGAGTTGTTAT; R26R-2, GCGAAGAGTTTGTCCTCAACC). *Tie2lacZ* (Schlaeger et al., 1997) -positive animals were identified by X-gal staining (see below) of tail biopsies before weaning. Noon on the day after mating (as judged by vaginal plug) was

designated as E0.5. Embryos were staged precisely by somite count and comparison with established references (Kaufman, 1992).

Gene expression assays and histology

RNA probes were labeled with digoxigenin (Roche) and used for whole-mount in situ hybridization according to standard protocols (Belo et al., 1997). All riboprobes were synthesized from published plasmids: *Tcfap2a* (Mitchell et al., 1991), *Crabp1* (Stoner and Gudas, 1989), cadherin 6 (Inoue et al., 1997), *Tcf21* (Quaggin et al., 1998). *lacZ* transgenes were visualized by fixing embryos for 15 minutes at room temperature with 4% paraformaldehyde, rinsed and stained overnight with X-gal stain. *Tie2-lacZ* embryos were cleared to benzyl alcohol: benzyl benzoate (BABB). Histological analysis was conducted on 8 μm paraffin wax-embedded sections using established protocols (Hogan et al., 1994). Section immunohistochemistry with antibodies for smooth muscle actin (Sigma clone 1A4) and PECAM1 (BD Pharmingen) used colorimetric substrates (NBT/BCIP). The WT1 antibody (Santa Cruz) was used on cryosections at 1:500 and visualized with AlexaFluor 594 Goat anti-Rabbit IgG (Molecular Probes) at 1:500. Whole-mount immunohistochemistry was carried out with 2H3 supernatant from the Developmental Studies Hybridoma Bank at the University of Iowa. Proliferating cells were marked with an antibody against phosphorylated histone H3 (Upstate Biotechnologies) at 1:1000 overnight at 4°C; Goat anti-Mouse Cy3 (Jackson) overnight at 4°C at 1:1000. Confocal microscopy utilized a Zeiss LSM 510. Mitotic indices were calculated as percent of labeled cells among the total number of DAPI counterstained cells (staining for 5 minutes at room temperature).

Ink injections

To analyze blood flow, dissected embryos were injected with India ink into the ventricle using a pulled capillary tube and mouth pipette. Embryos were subsequently fixed in paraformaldehyde and cleared in BABB (Hogan et al., 1994).

RT-PCR and PCR

To test for the presence of Cre, tissues were microdissected from embryos. RNA was purified using Trizol reagent and standard procedures, including DNAse treatment to prevent genomic DNA contamination (Sambrook and Russell, 2001). Total RNA was used for in vitro cDNA synthesis with MMLV reverse transcriptase (MMLV-RT; Gibco). Cre was amplified with the same primers as for genotyping. HPRT primers were used as published (Stottmann et al., 2001).

Results

Wnt1-Cre mediates *Bmpr1a* ablation from early stages of neural crest development, resulting in mid-gestational lethality

Our strategy for assessing the role of *Bmpr1a* in NCC development relied on the use of a conditional allele of *Bmpr1a* (Mishina et al., 2002) in concert with an established *Wnt1-Cre* transgene (Danielian et al., 1998) to drive recombination specifically in NCCs (Brault et al., 2001; Chai et al., 2000; Jiang et al., 2000). To visualize Cre activity in NCCs, *Wnt1-Cre* mice were crossed to a Cre recombination reporter line, R26R (Soriano, 1999). Recombination by Cre at the R26R locus brings a *lacZ* transgene under the irreversible control of a ubiquitous promoter. Embryos carrying *R26R* express *lacZ* in all cells that express active Cre recombinase, and in the descendents of those cells.

Recombination at the dorsal neural folds of the midbrain/hindbrain junction was visible by 4 s (Fig. 1A,B), reflecting a domain of *Wnt1* expression required for midbrain development (McMahon and Bradley, 1990). The first distinct NCCs were seen along the dorsal neural

folds of the hindbrain at the 5 s stage; these are more numerous by 6 s (Fig. 1C,D). Recombination extended into the rostral spinal cord by 8 s (Fig. 1E,F). Transverse sections of *Wnt-1Cre; R26R* embryos at ~10 s (E8.5) revealed migration from the neural tube to the pharyngeal arches and other target tissues (Fig. 1G and data not shown). Recombination then extended caudally along the dorsal neural tube to include the entire neural crest and its descendents (Fig. 1H,I). *Wnt1-Cre* activity in the neural crest at 5 s coincides with the time at which the first NCCs have been detected by cell labeling studies (Serbedzija et al., 1992). Thus, *Wnt1-Cre* allows recombination of *Bmpr1a* in the neural crest from very early stages of its development.

Mice carrying the *Wnt1-Cre* transgene and a null allele of *Bmpr1a* (*Bmpr1a*^{null}) were crossed to mice homozygous for a conditional allele of *Bmpr1a* (*Bmpr1a*^{flox}; Fig. 2A). One quarter of the resulting embryos are of the genotype *Wnt1-Cre; Bmpr1a*$^{flox/null}$, and are presumably unable to signal through BMPRIA in NCCs and their derivatives: we designate these as ‘mutant’. Simultaneous expression of the *Wnt1-Cre* transgene and the *Bmpr1a* conditional allele results in recombination at the *Bmpr1a* locus as intended (Fig. 2B; data not shown). Although we are unable to analyze precisely when BMPRIA ceases to function in any given NCC cell, our experimental system results in the removal of BMPRIA during all but the earliest stages of NCC development. Available antibodies against BMPRIA and the phosphorylated form of SMAD1 (indicating BMP signal transduction) proved ineffective in assessing BMPRIA protein and its output at the single-cell level (R.W.S. and J.K., unpublished). However, several previous studies with this conditional allele in a variety of contexts (Ahn et al., 2001;Gaussin et al., 2002;Hebert et al., 2002;Jamin et al., 2002;Mishina et al., 2002) have given no reason to suspect significant residual BMPRIA protein or incomplete *Bmpr1a*^{flox} recombination. Thus, although ablation of BMPRIA in the neural crest domain will not necessarily happen before the induction of the first NCCs, which must occur prior to 5 s in the hindbrain, the receptor is likely to be absent well before NCC generation is complete at any axial level. This occurs at 11 s at the earliest location, in the rostral hindbrain (Serbedzija et al., 1992), by which time expression of Cre has been robust for half a day. Moreover, BMPRIA should be absent in NCCs during their migration to target tissues and their differentiation upon arrival.

In dissections from the crosses to produce mutant embryos, *Wnt1-Cre; Bmpr1a*$^{flox/null}$ embryos were fully represented up to E11.5 (Fig. 2H,J), but did not survive beyond E12.5 (n=0/47; Fig. 2K; Table 1). At E.11.0, mutants looked externally normal and had normal circulation (Fig. 2E,F). By contrast, from E11.5, they showed evidence of severe circulatory defects (n>60). For example, yolk sacs appeared to contain no blood (Fig. 2I) and embryos displayed pooling of blood in major vessels, heart and liver (Fig. 2J). The majority of embryos recovered at E12.5 were clearly necrotic (Table 1). Thus, embryos lacking *Bmpr1a* in NCCs die abruptly with symptoms of acute heart failure around E11.5–12.0.

Neural crest cells are specified and differentiate in *Bmpr1a* neural crest mutants

Mutant embryos showed no deficit in NCC specification or migration from the neural tube, as assayed by expression of the neural crest markers *Tcfap2a* (*AP2α*: n=4), cadherin 6 (n=4) and *Crabp1* (n=3) at E9.5 and E10.5 (Fig. 3A,B). Initial differentiation also appeared normal; for example, an antibody marking neurofilaments of the peripheral nervous system indicated normal formation of sensory neurons (Fig. 3C,D). By including the recombination reporter *R26R* in our breeding scheme to ablate *Bmpr1a* in the neural crest, such that each resulting embryo carries one copy of *R26R*, we simultaneously mark both NCCs and cells lacking *Bmpr1a* (though we cannot be certain that any specific labeled cell necessarily lacks *Bmpr1a*, as the loxP sites in *R26R* and *Bmpr1a*^{flox} recombine independently). These NCC-labeled embryos showed that mutant cells achieved a normal distribution at E11.0 and integrated into many differentiating tissues and organs, such as pharyngeal arches and dorsal

root ganglia (Fig. 3E,F). Although assessing the ability of mutant NCCs to contribute to each neural crest derivative type is well beyond the scope of this study, it is clear that NCCs devoid of *Bmpr1a* can contribute normally to many tissues up through the time of embryonic death. Our experiments do not allow us to assess the requirement for BMPRIA during initial neural crest specification; nevertheless, the data show that *Bmpr1a* is not required in NCCs from early somite stages for any ongoing specification, nor for migration or differentiation into many derivative cell types.

Circulatory defects in *Bmpr1a* neural crest mutants

The appearance of mutant embryos at E11.5 indicated severe cardiovascular defects. Although we observed a loss of yolk sac circulation, we detected no NCC contribution to extra-embryonic tissues such as the yolk sac in either wild-type or mutant embryos (Fig. 4A). Moreover, yolk sac vessels appeared normal, as judged by histological analysis and by expression of the endothelial marker *Tie2-lacZ* (Fig. 4B). Thus, the effect of NCCs on the yolk sac blood flow is indirect. Embryonic peripheral vascular circulation in the mutants also appeared abnormal at E11.5, but did not show a structural defect in endothelium, as marked by the expression of *Tie2-lacZ* or by anti-PECAM1 (Fig. 4C–F). NCCs contribute to the supportive smooth muscle layer surrounding peripheral vasculature (Etchevers et al., 2001;Waldo et al., 1996;Willette et al., 1999). However, immunohistochemistry to label vascular smooth muscle cells in either pharyngeal arch arteries (Fig. 4G,H) or outflow tract tissue (Fig. 4I,J) showed no differences between wild-type and mutant embryos before the onset of embryonic necrosis. These data strongly suggest that the lack of yolk sac circulation and the frequent pooling of blood in the mutant (Fig. 2J) is a sign of impending death, secondary to a crucial cardiovascular deficit elsewhere in the embryo, such as inadequate blood flow from the heart.

Ablation of *Bmpr1a* in neural crest cells leads to outflow tract defects

NCCs are known to have an essential role in heart development: they migrate along the pharyngeal arch arteries to populate the outflow tract (OFT), where they are required for septation of the truncus arteriosus into the aorta and pulmonary artery (Kirby and Waldo, 1995). All mutant embryos analyzed (14) showed shortened OFTs and right ventricles as early as the 18 s stage when compared with stage-matched control embryos. Further analysis of mutant embryos carrying the *R26R* reporter showed reduced NCC contribution to the truncus arteriosus. This reduced NCC population and right ventricle shortening was observed at all stages examined from E9.0 (Fig. 5A–D, ~18 s) to E11.0 (Fig. 5I–L, 36–40 s). Shortened truncus arteriosus and right ventricle were present in mutant embryos past E11.0/40 s but these were excluded from analysis as the defect in the dying embryos could be a result of overall embryonic necrosis (data not shown). Shortened outflow tract tissue with reduced NCCs also lacked pronounced, well-formed endocardial cushions (Fig. 5M,N). Consistent with reduced NCC immigration, the *Tie2-lacZ* transgene marked the endothelium of the distinct aorta and pulmonary artery of wild-type embryos (Fig. 5Q), but revealed a lack of septation of the truncus arteriosus in mutants (arrow in Fig. 5R). Although the embryos observed at E12.0 were beginning to show signs of necrosis, their apparent lack of endocardial cushion formation is consistent with the findings of reduced NCCs and persistent truncus arteriosus.

We considered that a reduction in NCC migration to the OFT might result in occlusion of pharyngeal arch arteries by ectopic NCCs, which could potentially cause embryonic death at mid-gestation due to insufficient blood flow to the body. It is noteworthy that these mutant embryos also occasionally showed hypoplastic aortic arch arteries at E11.5 (Fig. 5T and data not shown). We tested the ability of the heart, great vessels and aortic arch arteries from *Bmpr1a* NCC mutants to allow unimpeded blood flow by injecting ink into the ventricles

and following its dispersal; we never detected any blockage or impeded flow (Fig. 5S,T). More importantly, we examined mutant and control embryos by serial histological sections of the entire OFT and pharyngeal arches at E11.5, and never observed blocked or occluded vessels (Fig. 5M–P). Even in a clearly necrotic embryo at E12.5 (Fig. 5V), sections through the outflow tract show a lack of septation and pooling of blood cells, but no ectopic tissues creating a barrier to blood flow to the peripheral tissues (Fig. 5U). OFT septation defects per se are not necessarily lethal until birth in chicks, mice or humans (Conway et al., 1997;Kirby and Waldo, 1995;Mair et al., 1992), and thus seem unlikely to account for the mid-gestational death we observed. These considerations led us to suspect that although the outflow tract defects might exacerbate circulatory deficiency, the primary problem in *Bmpr1a* neural crest mutants lies elsewhere.

Thin ventricular wall in *Bmpr1a* neural crest mutants

To elucidate the cause of the cardiovascular dysfunction and lethality in embryos lacking *Bmpr1a* in NCCs, we examined whether there might be defects in cardiac tissues not known to involve NCC contributions. Ventricular structure at E10.5 and E11.0 looked normal in mutant embryos (Fig. 6A–D) with formation of both the compact myocardium on the periphery of the ventricle, and the trabecular myocardium adjacent to the ventricular cavity. At E11.5, however, both layers were significantly reduced in mutants, showing a severely thinned compact myocardial wall and little expansion of the trabeculated myocardium relative to wild type (Fig. 6E–H). These defects were seen prior to the onset of embryonic necrosis (Fig. 6F).

Such dramatic changes in the morphology of ventricular tissue could be accomplished via a change in the amount of cell death or cell proliferation. Using the TUNEL assay to mark apoptotic cells in sectioned hearts, we detected no increase in myocardial cell death prior to global necrosis of mutant embryos (data not shown). By contrast, cell proliferation assays, using immunohistochemistry for phosphorylated histone H3 to mark cells in metaphase, revealed a dramatic difference in cell proliferation rates in the ventricular myocardium (Fig. 6I). Total myocardial proliferation in mutants was decreased 24% at E10.5 ($P<0.001$) and 21% at E11.5 ($P<0.001$), relative to stage-matched control embryos. When proliferating cells were tallied as a percentage of total cells in the ventricular myocardium to calculate a myocardial mitotic index, they were significantly reduced by this measure as well (2.93% in controls versus 1.63% in mutants, $P<0.015$).

A population of neural crest cell derivatives may colonize the epicardium

The mechanism by which the lack of a gene specifically in NCCs could lead to a deficient ventricular myocardium is unclear. To determine whether there might be a previously unknown NCC contribution to the mouse heart, we used *Wnt1-Cre; R26R* embryos to assess the distribution of NCC derivatives in and around the ventricles. Embryos at E9.5 showed a few β-galactosidase-positive cells immediately ventral to the heart and in the epicardium (Fig. 7A), a thin mesothelial tissue surrounding the heart. The epicardium derives primarily from cells on the posterior side of the septum transversum, which lies just caudal to the primitive ventricles. The epicardium expands to cover the ventricular surface in an epithelial sheet by E10.0 (Komiyama et al., 1987). Some of the epicardial cells undergo an epithelial-mesenchymal transition and contribute to several lineages within the heart, including connective tissue and coronary vascular elements (Munoz-Chapuli et al., 2002). In E10.5 and E11.5 *Wnt1-Cre; R26R* embryos, progressively more marked cells were seen in the epicardium, and also in the outer ventricular myocardium (Fig. 7B,C). No labeled cells were ever seen in the epicardium (or elsewhere) of *R26R* embryos lacking Cre; furthermore, the same distribution of stained cells is seen in *Wnt1-Cre; R26R* embryos regardless of whether they were processed for β-galactosidase activity and then sectioned, or sectioned and then

processed for activity (Fig. 7F). Together, these data eliminate the possibility that the labeled cells are artifacts of β-galactosidase staining. Although an epicardial NCC lineage has not been documented previously using this transgene, all other *Wnt1-Cre* lineages detected in our embryos are identical to those shown in previous studies (Jiang et al., 2000).

Importantly, in both wild-type and mutant embryos, most cells of the epicardium do not express the NCC lineage marker; the labeled epicardial population never exceeded 12% in any of our specimens. Moreover, we failed to detect labeled cells in the epicardium of some *Wnt1-Cre; R26R* embryos, despite equivalent staging, fixation and processing. We suspect the failure to observe these cells in all specimens reflects a technical limitation of our detection procedures.

Like other epicardial cells, a few of these lineage-labeled cells then invade the ventricular myocardium (Fig. 7F). Because cells of the epicardium populate the coronary arteries, we examined these vessels in late-gestation *Wnt1-Cre; R26R* embryos for the presence of labeled cells. We observed labeled cells in the coronary arteries in both whole-mount (Fig. 7D) and sectioned hearts (Fig. 7E). Collectively, this distribution of marked cells suggests that a small population of NCCs migrates to the epicardium, where it integrates into the nascent epicardial epithelium and has similar cell fates as neighboring epicardial cells from other origins.

We conducted additional tests to further evaluate the hypothesis that the labeled epicardial cells derive from the neural crest. First, we assessed the distribution of cells labeled by an independent NCC genetic lineage marker, *P0-Cre* (Yamauchi et al., 1999). *P0-Cre; R26R* embryos showed a similar contribution of NCCs to the epicardium and myocardium (Fig. 7G,H). We then considered whether these cells might reflect coincidental activity of *Wnt1-Cre* and *P0-Cre* transgenes in some novel domain outside the neural crest, such as the proepicardial organ or epicardium itself. To determine whether these cells could result from ectopic *Cre* expression outside the neural crest, we assayed tissue ventral to the neural tube, including the heart and all other thoracic tissues, for *Wnt1-Cre* expression by reverse transcription coupled to the polymerase chain reaction (RT-PCR). We found no Cre expression in ventral tissues collected from E9.5 and E10.5 *Wnt1-Cre* embryos, covering a wide range of somite numbers (0/37; Fig. 7I). We cannot exclude the possibility that there may be a brief burst of short-lived Cre expression in a temporal window not represented in our samples, although this seems unlikely. Instead, these data taken together strongly suggest that a small population of labeled epicardial and myocardial cells derive from the neural crest.

Among several BMPs expressed in the developing heart, BMP2 and BMP4 are known to be ligands for BMPRIA. BMP2 is expressed in the atrioventricular canal from E9 to E11 (Zhang and Bradley, 1996). Using a *Bmp4-lacZ* transgene (Lawson et al., 1999), we observed that *Bmp4* is expressed at high levels in the parietal pericardium of the thoracic body wall from E9.5 through E11.5 (Fig. 7J–L; data not shown). This suggests that at least one BMPRIA ligand, BMP4, is present in a cell population adjacent to potential receiving cells in the epicardium.

Intact epicardium in *Bmpr1a* neural crest mutants

We then assessed whether the epicardium might show abnormalities in *Bmpr1a* neural crest mutants. Examination of *Wnt1-Cre; Bmpr1a*^{flox}*; R26R* embryos revealed an indistinguishable distribution of labeled cells in the epicardium between mutant and wild-type embryos (Fig. 8A,B compared with Fig. 7A,B). This is in contrast to the truncus arteriosus, where there is a striking reduction in NCC population in mutants. Although mutant NCC derivatives populate the epicardium, it is conceivable nonetheless that the

epicardium is structurally abnormal in the mutants. Physical delay of migration of cells from the proepicardial organ results in a less extensive epicardial covering of the ventricles; this in turn is associated with reduced myocardial proliferation in underlying tissue (Perez-Pomares et al., 2002). To analyze the structure of the epicardium, we compared ventricular epicardium in sectioned mutant hearts and control littermates, and found no evidence for a disrupted or patchy epicardium (Fig. 8C–F). Moreover, the epicardial cell density in sections was not significantly different ($P>0.100$) between stage-matched mutant and wild-type embryos.

Although mutant embryos displayed a structurally intact epicardium, we assayed molecular markers of the epicardium to determine whether epicardial gene regulation is generally perturbed in the *Bmpr1a* neural crest mutants. In the heart, epicardin is expressed specifically in the epicardium (Robb et al., 1998). We detected no change in the expression of epicardin relative to wild type (Fig. 8G,H). WT1 is also expressed in the epicardium, but unlike epicardin, has been shown to have an important role in epicardial promotion of myocardial maturation (Kreidberg et al., 1993; Moore et al., 1999). Immunohistochemistry for the WT1 protein revealed no change in protein levels or localization between control and mutant embryos (Fig. 8I,J). Thus, the epicardium appears to be largely normal in mutant embryos.

Taken together, these data indicate that cells may migrate from the neural crest to the epicardium, where they are potentially exposed to several BMPs, including BMP4. Loss of *Bmpr1a* in NCCs results in midgestational defects in the underlying ventricular myocardium similar to those seen in epicardial ablations. The epicardial population of NCCs is distributed normally in mutant embryos, and the epicardium is structurally intact. These results therefore suggest a specific compromise in the proliferative influence of epicardium on ventricular myocardium upon loss of BMPRIA in neural crest derivatives.

Discussion

In this work, we sought to determine the requirements for BMPRIA signaling in neural crest cell development by ablating this receptor specifically in the neural crest domain from early somite stages. Although BMP 2/4 signaling promotes NCC induction, maintenance, delamination and migration from the neural tube (Aybar and Mayor, 2002; Knecht and Bronner-Fraser, 2002; LaBonne and Bronner-Fraser, 1999), embryos lacking *Bmpr1a* in forming NCCs show no discernable defects in these processes. However, these mutant embryos die of mid-gestational acute heart failure, with deficient ventricular myocardium proliferation and defective outflow tract morphogenesis.

Neural crest develops in the absence of BMPRIA

Although *Bmpr1a* is expressed throughout the neural plate, this receptor is dispensable for many aspects of NCC development. Definitive neural crest is first detectable at 5 s, beginning in the rostral hindbrain (Nichols, 1981), and production of NCCs is ongoing for ~9 hours at any given axial location, ending first in the hindbrain at 11 s to 14 s (Serbedzija et al., 1992). Meanwhile, *Wnt1-Cre* is expressed from 5 s in the hindbrain, and has been strongly expressed there for several hours by 11 s. Even if there were perdurance of BMPRIA protein long after the gene has been ablated (not suggested by previous studies with this allele), it seems unlikely that significant numbers of putative NCCs would retain BMPRIA protein during the whole window of NCC production. If the receptor were required for early NCC development but were not ablated soon enough, one would have expected that the initial NCCs would form and migrate away, but that continued production would decline and stop. Instead, we observed continuous production of NCCs indistinguishable from wild-type controls. Moreover, the BMPRIA protein would have been

absent for many hours as the NCCs migrate to target tissues and differentiate. It may be that the only crucial period for BMPRIA signaling occurs prior to 5–6 s, when *Wnt1-Cre* recombination becomes prevalent in the forming neural crest; our current experiment is unable to assess the necessity for this receptor during the earliest phases of NCC specification. Taken together, these considerations strongly suggest that BMPRIA signaling is unnecessary in vivo for neural crest delamination, migration and differentiation into most derivative cell types.

A potential implication of our results is that BMP signaling in general may not have an essential role in many aspects of mammalian NCC development. Neither of the other known BMP type I receptors, BMPRIB and ActRIa, is known to be expressed in the neural tube during early NCC development (Gu et al., 1999; Panchision et al., 2001; Yoshikawa et al., 2000). However, it remains possible that ectopic expression of *Bmpr1b* or *Actr1a*, or perhaps an unknown TGFβ family type I receptor, can compensate for the absence of *Bmpr1a* in this context.

BMP signaling in neural crest cells is required for outflow tract development

Our study reveals a critical requirement for BMPRIA signaling in proper formation and septation of the cardiac OFT. Although NCCs successfully migrate to the OFT in mutant embryos, we observed severe OFT defects, including a failure of septation and reduced conotruncal length. These phenotypes, which result from the ablation of a single gene product, closely resemble those resulting from physical ablation of the entire cardiac neural crest in chick embryos, roughly extending from the otic vesicle to the fourth somite (Kirby and Waldo, 1995). Further studies into the mechanism of the reduced OFT in cardiac NCC ablations reveal an accompanying defective migration of the outflow tract myocardium from an anterior heart field (Yelbuz et al., 2003). We see no evidence for a change in cell number through cell death or cell proliferation changes in the OFT of our mutant embryos. Therefore, we suggest that NCCs require BMPRIA for proper colonization of the OFT. Furthermore, we speculate that the NCCs colonizing the OFT in wild-type embryos may secrete a factor downstream of BMPRIA signal transduction, lacking in our mutants, that stimulates migration of future outflow tract myocardial cells from the secondary heart field to form a fully mature OFT and right ventricle (Kelly et al., 2001; Mjaatvedt et al., 2001; Waldo et al., 2001).

Although other organogenesis defects also result from cardiac neural crest ablations, such as deficient thymus and parathyroid, the *Bmpr1a* mutant embryos studied here died too soon (prior to E12.5) to address whether BMPR1A in NCCs is required for development of these organs. Nevertheless, our results complement earlier genetic evidence that BMP signaling is necessary for OFT septation. A hypomorphic allele of the gene encoding BMPRII, the binding partner of BMPRIA, also results in OFT defects (Delot et al., 2003). Overexpression of the BMP antagonist Noggin in chick heart and great vessels, expected to decrease effective BMP ligand levels in these tissues, results in OFT septation anomalies as well (Allen et al., 2001). In both the chick Noggin cardiac misexpression experiments and the mouse NCC *Bmpr1a* ablation studies, NCCs entered the OFT but failed to migrate as far towards the ventricles as in control embryos. Several BMP ligands are expressed in the early OFT, including BMP2, BMP4, BMP6 and BMP7 (Bitgood and McMahon, 1995; Jones et al., 1991; Kim et al., 2001; Lyons et al., 1990). Together, these considerations suggest that local BMPs in and around the conotruncus signal through BMPRIA in the incoming NCCs to promote myocardial morphogenesis and NCC colonization of the septating truncus arteriosus.

The acute heart failure observed just before death of the *Wnt1-Cre;Bmpr1a*$^{flox/null}$ embryos was not due to a failure of blood to flow through the OFT to the periphery. Persistent

(unseptated) truncus arteriosus is not necessarily lethal until birth, when the fetus requires distinct pulmonary and systemic circulations. Although the aortic arch arteries were occasionally somewhat hypoplastic in the mutants and may have reduced flow, the lumens of neither these arteries nor the truncus arteriosus were occluded. Indeed, other mutants with hypoplastic aortic arch arteries survive beyond E12.5 (Abu-Issa et al., 2002; Lindsay and Baldini, 2001; Yanagisawa et al., 2003), by which time the *Bmpr1a* NCC mutants have died.

BMPRIA functions outside the ventricular myocardium to promote its proliferation

The primary cause of death in the *Wnt1-Cre; Bmpr1a* mutants is ventricular dysfunction and a consequent failure to pump an adequate supply of blood. The lethal phase is very narrow: mutants occur at Mendelian levels (25%) at E11, but are entirely absent by E13. The ventricular myocardium appears reduced shortly before death, particularly the outer, compact layer. Although the ventricles of mutant embryos look normal through E11.0, the ventricular myocardium shows significantly reduced cell proliferation by E10.5.

The thin-walled ventricular myocardial phenotype that we observe resembles phenotypes reported for loss-of-function mutations in several other mouse loci. These include the genes encoding WT1 (Kreidberg et al., 1993), RARα (Kastner et al., 1997), RXRα (Sucov et al., 1994), α4 integrin (Yang et al., 1995), VCAM1 (Kwee et al., 1995), FOG2 (Tevosian et al., 2000), erythropoietin and the erythropoietin receptor (Wu et al., 1999), and others. These mutants are all general ‘knockout’ mutations, in which the entire embryo has deficient gene activity. By contrast, our ablation of *Bmpr1a* was restricted to a very limited extracardiac population, with *Bmpr1a* activity intact in myocardial cells. Thus, the myocardial phenotype is caused indirectly, specifically as a result of deficient BMP signaling in an extracardiac cell population that must function in a tissue interaction that regulates myocardial proliferation in the ventricles.

A small cell population in the epicardium that signals through BMPRIA may promote ventricular proliferation

We observed a novel population of labeled cells contributing to the epicardium from E9.5, and propose that deficient BMPRIA activity in this lineage is responsible for the ventricular defects. Considerable genetic evidence suggests that a defective epicardium can lead to reduced myocardial proliferation. For example, *Wt1* is expressed in epicardium, but not in myocardium, yet has a very similar thin compact myocardium phenotype; expression of *Wt1* specifically in the epicardium rescued the thin-walled phenotype and death (Moore et al., 1999). Interference with retinoic acid signaling in the epicardium mimicked the thin-walled myocardium phenotype of *Rxra* mutant embryos (Chen et al., 2002). In the VCAM1, FOG2 and α-4integrin mutants, the tight juxtaposition of epicardium with ventricular myocardium was abnormal, with corresponding thinning of the myocardium (Kwee et al., 1995; Tevosian et al., 2000; Yang et al., 1995). Embryological studies complement these results. Ablation of the proepicardial organ has a similar phenotype, and reduced migration to the heart results in patchy epicardium with reduced ventricular myocardium thickness underlying the deficient areas of the epicardium (Gittenberger-de Groot et al., 2000; Perez-Pomares et al., 2002; Poelmann et al., 2002). This reduction in ventricular wall thickness resulting from interference with the epicardium is caused primarily by reduced cell proliferation (Pennisi et al., 2002).

Thus, the thin-walled ventricular phenotype we observe in *Wnt1-Cre;Bmpr1a* mutants is very similar to those resulting from molecular or structural epicardial defects. Our analysis indicated that the epicardium in the mutants has no detectable structural problems, and that the expression of at least some epicardial markers was normal. Moreover, we found that the epicardial population of recombined (labeled) cells was indistinguishable between mutants

and wild-type littermates. These data suggest that the relevant defect in the mutants is the specific lack of functional BMPRIA in this population of epicardial cells.

Two recent studies have demonstrated directly that the epicardium produces secreted factors that promote proliferation of the underlying ventricular myocardium. Chen and colleagues (Chen et al., 2002) found that cultured mouse epicardial cells produce trophic factors for myocardial cell proliferation, and production of this trophic activity depends on retinoid signal transduction in the epicardial cells. Stuckmann et al. (Stuckmann et al., 2003) also found that blocking retinoid signaling in the epicardium blocks production of a secreted myocardial proliferation factor, as does blocking erythropoietin signaling. Neither study identified the proliferation factor(s) produced by epicardial cells.

Our data lead us to propose a model for an essential role of BMPRIA signaling in an epicardial cell population in promoting ventricular development (Fig. 9A–C). An extracardiac lineage of cells (reflecting *Wnt1-Cre* recombination) migrates to the epicardium, and via BMPRIA transduces a BMP signal. We found that BMP4 (a known ligand) is expressed at high levels in cells adjoining the epicardium, though other work has demonstrated expression of *Bmp5*, *Bmp6*, *Bmp7* and *Bmp10* in the myocardium at many stages (Dudley and Robertson, 1997; Kim et al., 2001; Neuhaus et al., 1999; Solloway and Robertson, 1999). Transduction of BMP signals by BMPRIA in these epicardial cells would in turn stimulate production within the epicardium of an unidentified proliferation signal for the underlying ventricular myocardium. As we can detect only a limited contribution of recombined cells to the epicardium, this population probably acts upon other cells of the epicardium to stimulate production of this myocardial proliferation signal(s). Thus, a limited number of recombined cells may lead to a defect in signaling from a much larger region of the epicardium. As a result, the *Wnt1-Cre; Bmpr1a*$^{flox/null}$ embryos would produce reduced proliferation signal(s) and consequently experience a critical underproliferation of the ventricular myocardium. Reduced compact and trabeculated myocardium precludes sufficient blood flow for the metabolic demands of the rapidly growing embryo. Embryonic lethality then results primarily from ventricular failure, caused by deficient myocardial maturation. The ventricular deficiency of the mutants analyzed here may be compounded by restricted flow through the unseptated outflow tract and hypoplastic aortic arch arteries. Within the ventricular myocardium itself, BMPRIA has been proposed to transduce a myocyte growth signal (Gaussin et al., 2002), though in our mutants the myocardium per se is wild type.

An alternative model for the defective ventricular proliferation we observed in the *Wnt1-Cre; Bmpr1a*$^{flox/null}$ embryos involves the NCCs that migrate around the pharyngeal tissues to populate the outflow tract (Fig. 9D,E). We observed that the colonization of the developing OFT by NCCs was much reduced when these cells lacked BMPRIA; notably, the NCC population extended much less far down the OFT toward the ventricles. It is possible that NCC derivatives colonizing the OFT require BMPRIA for production of a secreted mitogen for the myocardium. In the absence of the receptor, there would be less of this mitogen produced, with a consequent under-proliferation of the myocardium. Some evidence consistent with this model comes from studies in the chicken, where NCC ablation leads to defective ventricular myocardium (Waldo et al., 1999). Although the resulting phenotypes varied widely and showed a general increase in myocardial proliferation (in contrast to the consistently reduced proliferation observed here), these results support the view that the neural crest in some way exerts an early influence on organization of the ventricular myocardium. A molecular mechanism for this influence is difficult to envision, in that it must involve very long-range signaling. However, direct co-culture of the myocardium with ventral pharynx (i.e. without NCCs) resulted in changes in myocardial Ca^{2+} signaling and increased proliferation (Farrell et al., 1999); this action of the pharynx

was repressed by FGF function blocking antibody. This may indicate that signaling from the pharynx has a negative effect on myocardial development, mediated by FGFs, that is normally alleviated by NCCs as they colonize the pharyngeal arches and OFT. To extrapolate this model to the experimental situation studied here, one might envision that reduced NCC migration into the developing OFT in the *Wnt1-Cre; Bmpr1a*$^{flox/null}$ embryos allows more pharyngeal FGF to perturb ventricular development. Although we cannot rule out such an interaction between NCCs in the pharynx and FGF (or other) signals, we suggest that a disrupted epicardial signaling cascade is a more likely cause of the myocardial proliferation defect seen in our mutants.

Is there a neural crest contribution to the epicardium?

Although *Wnt1-Cre* expression has been associated exclusively with the neural crest and its derivatives (Brault et al., 2001; Chai et al., 2000; Jiang et al., 2000), the epicardium of *Wnt1-Cre; R26R* embryos contained a small proportion of recombined cells. This indicates that they are derived from a Cre-expressing lineage. Although we were unable to detect such cells in every specimen (probably for technical reasons), control experiments indicated that the labeling was not a staining artifact. These labeled cells later populated the same tissues as epicardial derivatives (coronary arteries and scattered cells in the ventricular wall). Because these epicardial cells clearly underwent epithelial-mesenchymal transition (EMT) to clonally populate these structures, it is possible that this population represents a fraction of the epicardium that is competent to undergo EMT rather than remaining an obligate part of the epicardial mesothelium.

We observed a *Wnt1-Cre* lineage of cells in the septum transversum adjacent to the ventricles at E9.5. This is the location of the proepicardial organ, the source of epicardial cells. We therefore suspect that the labeled cells of the epicardium came from this tissue, though it is also possible that they have migrated in from a known neural crest domain elsewhere. We are uncertain whether these labeled cells are of neural crest origin, or if they represent a hitherto undetected independent expression domain of *Wnt1-Cre*. However, we saw exactly the same distribution of labeled cells when we used *PO-Cre* as an independent neural crest lineage marker. Moreover, using the sensitive assay of RT-PCR, we never detected Cre expression in non-dorsal tissues dissected from *Wnt1-Cre* embryos from E9.5–10.5 (during which time the epicardium forms). These considerations lead us to suspect that the labeled epicardial cells are of neural crest origin, though they probably arrive via the proepicardial organ.

Although an epicardial NCC lineage has not been otherwise observed in mice or chicks, recent evidence suggests NCCs contribute to ventricular myocardium in zebrafish (Li et al., 2003; Sato and Yost, 2003). In mice and chickens with NCC defects, myocardial defects are seen before NCCs are known to populate the outflow tract, suggesting that NCCs produce factor(s) involved in myocardial development (Creazzo et al., 1998). Moreover, *Pax3* expression in NCCs rescues the reduced myocardial tissue phenotype of *Pax3*-null mutants (Li et al., 1999). We suggest that lesions in an early population of NCC derivatives, migrating into the epicardium and/or outflow tract, account for previously observed myocardial defects associated with neural crest perturbations. Overall, our work demonstrates that BMPRIA is dispensable for most aspects of early neural crest development, and identifies a novel, crucial role for BMPRIA signal transduction in extra-cardiac cells during the development of the outflow tract and ventricular myocardium of the heart.

Acknowledgments

We thank B. Hogan and the anonymous reviewers of an earlier draft for helpful comments on the manuscript, and M. Kirby for insightful discussions. M. Berrong, J. Goodwin and A. Lawrence provided technical assistance. Mouse strains were generously provided by B. Hogan (*Bmp4-lacZ*), A. McMahon (*Wnt1-Cre*), P. Soriano (*R26R*) and K. Yamamura (*PO-Cre*). The 2H3 antibody, developed by J. Dodd and T. Jessell, was obtained from the Developmental Studies Hybridoma Bank maintained by the University of Iowa, Department of Biological Sciences, Iowa City, IA 52242. R.W.S. is supported by an NINDS fellowship (NS42486). This work was supported by NIH grants to J.K. (HD39948 and DE13674).

References

Abu-Issa R, Smyth G, Smoak I, Yamamura K, Meyers EN. Fgf8 is required for pharyngeal arch and cardiovascular development in the mouse. Development 2002;129:4613–4625. [PubMed: 12223417]

Ahn K, Mishina Y, Hanks MC, Behringer RR, Crenshaw EB 3rd. BMPR-IA signaling is required for the formation of the apical ectodermal ridge and dorsal-ventral patterning of the limb. Development 2001;128:4449–4461. [PubMed: 11714671]

Allen SP, Bogardi JP, Barlow AJ, Mir SA, Qayyum SR, Verbeek FJ, Anderson RH, Francis-West PH, Brown NA, Richardson MK. Misexpression of noggin leads to septal defects in the outflow tract of the chick heart. Dev. Biol 2001;235:98–109. [PubMed: 11412030]

Aybar MJ, Mayor R. Early induction of neural crest cells: lessons learned from frog, fish and chick. Curr. Opin. Genet. Dev 2002;12:452–458. [PubMed: 12100892]

Belo JA, Bouwmeester T, Leyns L, Kertesz N, Gallo M, Follettie M, de Robertis EM. Cerberus-like is a secreted factor with neutralizing activity expressed in the anterior primitive endoderm of the mouse gastrula. Mech. Dev 1997;68:45–57. [PubMed: 9431803]

Bitgood MJ, McMahon AP. Hedgehog and Bmp genes are coexpressed at many diverse sites of cell-cell interaction in the mouse embryo. Dev. Biol 1995;172:126–138. [PubMed: 7589793]

Brault V, Moore R, Kutsch S, Ishibashi M, Rowitch DH, McMahon AP, Sommer L, Boussadia O, Kemler R. Inactivation of the beta-catenin gene by Wnt1-Cre-mediated deletion results in dramatic brain malformation and failure of craniofacial development. Development 2001;128:1253–1264. [PubMed: 11262227]

Chai Y, Jiang X, Ito Y, Bringas P Jr, Han J, Rowitch DH, Soriano P, McMahon AP, Sucov HM. Fate of the mammalian cranial neural crest during tooth and mandibular morphogenesis. Development 2000;127:1671–1679. [PubMed: 10725243]

Chen TH, Chang TC, Kang JO, Choudhary B, Makita T, Tran CM, Burch JB, Eid H, Sucov HM. Epicardial induction of fetal cardiomyocyte proliferation via a retinoic acid-inducible trophic factor. Dev. Biol 2002;250:198–207. [PubMed: 12297106]

Christiansen JH, Coles EG, Wilkinson DG. Molecular control of neural crest formation, migration and differentiation. Curr. Opin. Cell Biol 2000;12:719–724. [PubMed: 11063938]

Conway SJ, Godt RE, Hatcher CJ, Leatherbury L, Zolotouchnikov VV, Brotto MA, Copp AJ, Kirby ML, Creazzo TL. Neural crest is involved in development of abnormal myocardial function. J. Mol. Cell Cardiol 1997;29:2675–2685. [PubMed: 9344762]

Creazzo TL, Godt RE, Leatherbury L, Conway SJ, Kirby ML. Role of cardiac neural crest cells in cardiovascular development. Annu. Rev. Physiol 1998;60:267–286. [PubMed: 9558464]

Danielian PS, Muccino D, Rowitch DH, Michael SK, McMahon AP. Modification of gene activity in mouse embryos in utero by a tamoxifen-inducible form of Cre recombinase. Curr. Biol 1998;8:1323–1326. [PubMed: 9843687]

Delot EC, Bahamonde ME, Zhao M, Lyons KM. BMP signaling is required for septation of the outflow tract of the mammalian heart. Development 2003;130:209–220. [PubMed: 12441304]

Dudley AT, Robertson EJ. Overlapping expression domains of bone morphogenetic protein family members potentially account for limited tissue defects in BMP7 deficient embryos. Dev. Dyn 1997;208:349–362. [PubMed: 9056639]

Etchevers HC, Vincent C, le Douarin NM, Couly GF. The cephalic neural crest provides pericytes and smooth muscle cells to all blood vessels of the face and forebrain. Development 2001;128:1059–1068. [PubMed: 11245571]

Farrell M, Waldo K, Li YX, Kirby ML. A novel role for cardiac neural crest in heart development. Trends Cardiovasc. Med 1999;9:214–220. [PubMed: 10881754]

Gaussin V, van de Putte T, Mishina Y, Hanks MC, Zwijsen A, Huylebroeck D, Behringer RR, Schneider MD. Endocardial cushion and myocardial defects after cardiac myocyte-specific conditional deletion of the bone morphogenetic protein receptor ALK3. Proc. Natl. Acad. Sci. USA 2002;99:2878–2883. [PubMed: 11854453]

Gittenberger-de Groot AC, Vrancken Peeters MP, Bergwerff M, Mentink MM, Poelmann RE. Epicardial outgrowth inhibition leads to compensatory mesothelial outflow tract collar and abnormal cardiac septation and coronary formation. Circ. Res 2000;87:969–971. [PubMed: 11090540]

Gu Z, Reynolds EM, Song J, Lei H, Feijen A, Yu L, He W, MacLaughlin DT, van den Eijnden-van Raaij J, Donahoe PK, et al. The type I serine/threonine kinase receptor ActRIA (ALK2) is required for gastrulation of the mouse embryo. Development 1999;126:2551–2561. [PubMed: 10226013]

Hebert JM, Mishina Y, McConnell SK. BMP signaling is required locally to pattern the dorsal telencephalic midline. Neuron 2002;35:1029–1041. [PubMed: 12354394]

Hogan, B.; Beddington, R.; Costantini, F.; Lacy, E. Manipulating the Mouse Embryo. New York: Cold Spring Harbor Press; 1994.

Inoue T, Chisaka O, Matsunami H, Takeichi M. Cadherin-6 expression transiently delineates specific rhombomeres, other neural tube subdivisions, and neural crest subpopulations in mouse embryos. Dev. Biol 1997;183:183–194. [PubMed: 9126293]

Jamin SP, Arango NA, Mishina Y, Hanks MC, Behringer RR. Requirement of Bmpr1a for Mullerian duct regression during male sexual development. Nat. Genet 2002;32:408–410. [PubMed: 12368913]

Jiang X, Rowitch DH, Soriano P, McMahon AP, Sucov HM. Fate of the mammalian cardiac neural crest. Development 2000;127:1607–1616. [PubMed: 10725237]

Jones CM, Lyons KM, Hogan BL. Involvement of Bone Morphogenetic Protein-4 (BMP-4) and Vgr-1 in morphogenesis and neurogenesis in the mouse. Development 1991;111:531–542. [PubMed: 1893873]

Kanzler B, Foreman RK, Labosky PA, Mallo M. BMP signaling is essential for development of skeletogenic and neurogenic cranial neural crest. Development 2000;127:1095–1104. [PubMed: 10662648]

Kastner P, Messaddeq N, Mark M, Wendling O, Grondona JM, Ward S, Ghyselinck N, Chambon P. Vitamin A deficiency and mutations of RXRalpha, RXRbeta and RARalpha lead to early differentiation of embryonic ventricular cardiomyocytes. Development 1997;124:4749–4758. [PubMed: 9428411]

Kaufman, MH. The Atlas of Mouse Development. San Diego: Academic Press; 1992.

Kawabata M, Imamura T, Miyazono K. Signal transduction by bone morphogenetic proteins. Cytokine Growth Factor Rev 1998;9:49–61. [PubMed: 9720756]

Kelly RG, Brown NA, Buckingham ME. The arterial pole of the mouse heart forms from Fgf10-expressing cells in pharyngeal mesoderm. Dev. Cell 2001;1:435–440. [PubMed: 11702954]

Kim RY, Robertson EJ, Solloway MJ. Bmp6 and Bmp7 are required for cushion formation and septation in the developing mouse heart. Dev. Biol 2001;235:449–466. [PubMed: 11437450]

Kirby ML, Waldo KL. Neural crest and cardiovascular patterning. Circ. Res 1995;77:211–215. [PubMed: 7614707]

Knecht AK, Bronner-Fraser M. Induction of the neural crest: a multigene process. Nat. Rev. Genet 2002;3:453–461. [PubMed: 12042772]

Komiyama M, Ito K, Shimada Y. Origin and development of the epicardium in the mouse embryo. Anat. Embryol 1987;176:183–189. [PubMed: 3619072]

Kreidberg JA, Sariola H, Loring JM, Maeda M, Pelletier J, Housman D, Jaenisch R. WT-1 is required for early kidney development. Cell 1993;74:679–691. [PubMed: 8395349]

Kwee L, Burns DK, Rumberger JM, Norton C, Wolitzky B, Terry R, Lombard-Gillooly KM, Shuster DJ, Kontgen F, Stewart C, et al. Creation and characterization of E-selectin- and VCAM-1-deficient mice. Ciba Found. Symp 1995;189:17–28. [PubMed: 7587631]

LaBonne C, Bronner-Fraser M. Molecular mechanisms of neural crest formation. Annu. Rev. Cell Dev. Biol 1999;15:81–112. [PubMed: 10611958]

Lawson KA, Dunn NR, Roelen BA, Zeinstra LM, Davis AM, Wright CV, Korving JP, Hogan BL. Bmp4 is required for the generation of primordial germ cells in the mouse embryo. Genes Dev 1999;13:424–436. [PubMed: 10049358]

Le Douarin, NM.; Kalcheim, C. The Neural Crest. New York: Cambridge University Press; 1999.

Li J, Liu KC, Jin F, Lu MM, Epstein JA. Transgenic rescue of congenital heart disease and spina bifida in Splotch mice. Development 1999;126:2495–2503. [PubMed: 10226008]

Li YX, Zdanowicz M, Young L, Kumiski D, Leatherbury L, Kirby ML. Cardiac neural crest in zebrafish embryos contributes to myocardial cell lineage and early heart function. Dev. Dyn 2003;226:540–550. [PubMed: 12619138]

Lindsay EA, Baldini A. Recovery from arterial growth delay reduces penetrance of cardiovascular defects in mice deleted for the DiGeorge syndrome region. Hum. Mol. Genet 2001;10:997–1002. [PubMed: 11309372]

Lyons KM, Pelton RW, Hogan BL. Organogenesis and pattern formation in the mouse: RNA distribution patterns suggest a role for bone morphogenetic protein-2A (BMP-2A). Development 1990;109:833–844. [PubMed: 2226202]

Mair, D.; Edwards, W.; Fuster, V.; Seward, J.; Danielson, G. Paediatric Cardiology. Vol. Vol. 2. Edinburgh: Churchill Livingstone; 1992. Truncus arteriosus and aortopulmonary window; p. 913-929.

McMahon AP, Bradley A. The Wnt-1 (int-1) proto-oncogene is required for development of a large region of the mouse brain. Cell 1990;62:1073–1085. [PubMed: 2205396]

Mishina Y, Hanks MC, Miura S, Tallquist MD, Behringer RR. Generation of Bmpr/Alk3 conditional knockout mice. Genesis 2002;32:69–72. [PubMed: 11857780]

Mishina Y, Suzuki A, Ueno N, Behringer RR. Bmpr encodes a type I bone morphogenetic protein receptor that is essential for gastrulation during mouse embryogenesis. Genes Dev 1995;9:3027–3037. [PubMed: 8543149]

Mitchell PJ, Timmons PM, Hebert JM, Rigby PW, Tjian R. Transcription factor AP-2 is expressed in neural crest cell lineages during mouse embryogenesis. Genes Dev 1991;5:105–119. [PubMed: 1989904]

Miyazono K, Kusanagi K, Inoue H. Divergence and convergence of TGF-beta/BMP signaling. J. Cell Physiol 2001;187:265–276. [PubMed: 11319750]

Mjaatvedt CH, Nakaoka T, Moreno-Rodriguez R, Norris RA, Kern MJ, Eisenberg CA, Turner D, Markwald RR. The outflow tract of the heart is recruited from a novel heart-forming field. Dev. Biol 2001;238:97–109. [PubMed: 11783996]

Moore AW, McInnes L, Kreidberg J, Hastie ND, Schedl A. YAC complementation shows a requirement for Wt1 in the development of epicardium, adrenal gland and throughout nephrogenesis. Development 1999;126:1845–1857. [PubMed: 10101119]

Munoz-Chapuli R, Macias D, Gonzalez-Iriarte M, Carmona R, Atencia G, Perez-Pomares JM. The epicardium and epicardial-derived cells: multiple functions in cardiac development. Rev. Esp. Cardiol 2002;55:1070–1082. [PubMed: 12383393]

Neuhaus H, Rosen V, Thies RS. Heart specific expression of mouse BMP-10 a novel member of the TGF-beta superfamily. Mech. Dev 1999;80:181–184. [PubMed: 10072785]

Nguyen VH, Schmid B, Trout J, Connors SA, Ekker M, Mullins MC. Ventral and lateral regions of the zebrafish gastrula, including the neural crest progenitors, are established by a bmp2b/swirl pathway of genes. Dev. Biol 1998;199:93–110. [PubMed: 9676195]

Nichols DH. Neural crest formation in the head of the mouse embryo as observed using a new histological technique. J. Embryol. Exp. Morphol 1981;64:105–120. [PubMed: 7031165]

Panchision DM, Pickel JM, Studer L, Lee SH, Turner PA, Hazel TG, McKay RD. Sequential actions of BMP receptors control neural precursor cell production and fate. Genes Dev 2001;15:2094–2110. [PubMed: 11511541]

Pennisi DJ, Rentschler S, Gourdie RG, Fishman GI, Mikawa T. Induction and patterning of the cardiac conduction system. Int. J. Dev. Biol 2002;46:765–775. [PubMed: 12382942]

Perez-Pomares JM, Phelps A, Sedmerova M, Carmona R, Gonzalez-Iriarte M, Munoz-Chapuli R, Wessels A. Experimental studies on the spatiotemporal expression of WT1 and RALDH2 in the embryonic avian heart: a model for the regulation of myocardial and valvuloseptal development by epicardially derived cells (EPDCs). Dev. Biol 2002;247:307–326. [PubMed: 12086469]

Poelmann RE, Lie-Venema H, Gittenberger-de Groot AC. The role of the epicardium and neural crest as extracardiac contributors to coronary vascular development. Tex. Heart Inst. J 2002;29:255–261. [PubMed: 12484609]

Quaggin SE, Vanden Heuvel GB, Igarashi P. Pod-1, a mesoderm-specific basic-helix-loop-helix protein expressed in mesenchymal and glomerular epithelial cells in the developing kidney. Mech. Dev 1998;71:37–48. [PubMed: 9507058]

Robb L, Mifsud L, Hartley L, Biben C, Copeland NG, Gilbert DJ, Jenkins NA, Harvey RP. epicardin: A novel basic helix-loop-helix transcription factor gene expressed in epicardium, branchial arch myoblasts, and mesenchyme of developing lung, gut, kidney, and gonads. Dev. Dyn 1998;213:105–113. [PubMed: 9733105]

Sambrook, J.; Russell, D. Molecular Cloning: A Laboratory Manual. Cold Spring Harbor Laboratory Press; 2001.

Sato M, Yost HJ. Cardiac neural crest contributes to cardiomyogenesis in zebrafish. Dev. Biol 2003;257:127–139. [PubMed: 12710962]

Schlaeger TM, Bartunkova S, Lawitts JA, Teichmann G, Risau W, Deutsch U, Sato TN. Uniform vascular-endothelial-cell-specific gene expression in both embryonic and adult transgenic mice. Proc. Natl. Acad. Sci. USA 1997;94:3058–3063. [PubMed: 9096345]

Serbedzija GN, Bronner-Fraser M, Fraser SE. Vital dye analysis of cranial neural crest cell migration in the mouse embryo. Development 1992;116:297–307. [PubMed: 1283734]

Solloway MJ, Robertson EJ. Early embryonic lethality in Bmp5; Bmp7 double mutant mice suggests functional redundancy within the 60A subgroup. Development 1999;126:1753–1768. [PubMed: 10079236]

Soriano P. Generalized lacZ expression with the ROSA26 Cre reporter strain. Nat. Genet 1999;21:70–71. [PubMed: 9916792]

Stoner CM, Gudas LJ. Mouse cellular retinoic acid binding protein: cloning, complementary DNA sequence, and messenger RNA expression during the retinoic acid- induced differentiation of F9 wild type and RA-3-10 mutant teratocarcinoma cells. Cancer Res 1989;49:1497–1504. [PubMed: 2538228]

Stottmann RW, Anderson RM, Klingensmith J. The BMP antagonists Chordin and Noggin have essential but redundant roles in mouse mandibular outgrowth. Dev. Biol 2001;240:457–473. [PubMed: 11784076]

Stuckmann I, Evans S, Lassar DB. Erythropoietin and retinoic acid, secreted from the epicardium, are required for cardiac myocyte proliferation. Dev. Biol 2003;255:334–349. [PubMed: 12648494]

Sucov HM, Dyson E, Gumeringer CL, Price J, Chien KR, Evans RM. RXR alpha mutant mice establish a genetic basis for vitamin A signaling in heart morphogenesis. Genes Dev 1994;8:1007–1018. [PubMed: 7926783]

Tevosian SG, Deconinck AE, Tanaka M, Schinke M, Litovsky SH, Izumo S, Fujiwara Y, Orkin SH. FOG-2, a cofactor for GATA transcription factors, is essential for heart morphogenesis and development of coronary vessels from epicardium. Cell 2000;101:729–739. [PubMed: 10892744]

Waldo KL, Kumiski D, Kirby ML. Cardiac neural crest is essential for the persistence rather than the formation of an arch artery. Dev. Dyn 1996;205:281–292. [PubMed: 8850564]

Waldo K, Zdanowicz M, Burch J, Kumiski DH, Stadt HA, Godt RE, Creazzo TL, Kirby ML. A novel role for cardiac neural crest in heart development. J. Clin. Invest 1999;103:1499–1507. [PubMed: 10359559]

Waldo KL, Kumiski DH, Wallis KT, Stadt HA, Hutson MR, Platt DH, Kirby ML. Conotruncal myocardium arises from a secondary heart field. Development 2001;128:3179–3188. [PubMed: 11688566]

Willette RN, Gu JL, Lysko PG, Anderson KM, Minehart H, Yue T. BMP-2 gene expression and effects on human vascular smooth muscle cells. J. Vasc. Res 1999;36:120–125. [PubMed: 10213907]

Wu H, Lee SH, Gao J, Liu X, Iruela-Arispe ML. Inactivation of erythropoietin leads to defects in cardiac morphogenesis. Development 1999;126:3597–3605. [PubMed: 10409505]

Yamauchi Y, Abe K, Mantani A, Hitoshi Y, Suzuki M, Osuzu F, Kuratani S, Yamamura K. A novel transgenic technique that allows specific marking of the neural crest cell lineage in mice. Dev. Biol 1999;212:191–203. [PubMed: 10419695]

Yanagisawa H, Clouthier DE, Richardson JA, Charite J, Olson EN. Targeted deletion of a branchial arch-specific enhancer reveals a role of dHAND in craniofacial development. Development 2003;130:1069–1078. [PubMed: 12571099]

Yang JT, Rayburn H, Hynes RO. Cell adhesion events mediated by alpha 4 integrins are essential in placental and cardiac development. Development 1995;121:549–560. [PubMed: 7539359]

Yelbuz TM, Waldo KL, Zhang X, Zdanowicz M, Parker J, Creazzo TL, Johnson GA, Kirby ML. Myocardial volume and organization are changed by failure of addition of secondary heart field myocardium to the cardiac outflow tract. Dev. Dyn 2003;228:152–160. [PubMed: 14517987]

Yoshikawa SI, Aota S, Shirayoshi Y, Okazaki K. The ActR-I activin receptor protein is expressed in notochord, lens placode and pituitary primordium cells in the mouse embryo. Mech. Dev 2000;91:439–444. [PubMed: 10704880]

Zhang H, Bradley A. Mice deficient for BMP2 are nonviable and have defects in amnion/chorion and cardiac development. Development 1996;122:2977–2986. [PubMed: 8898212]

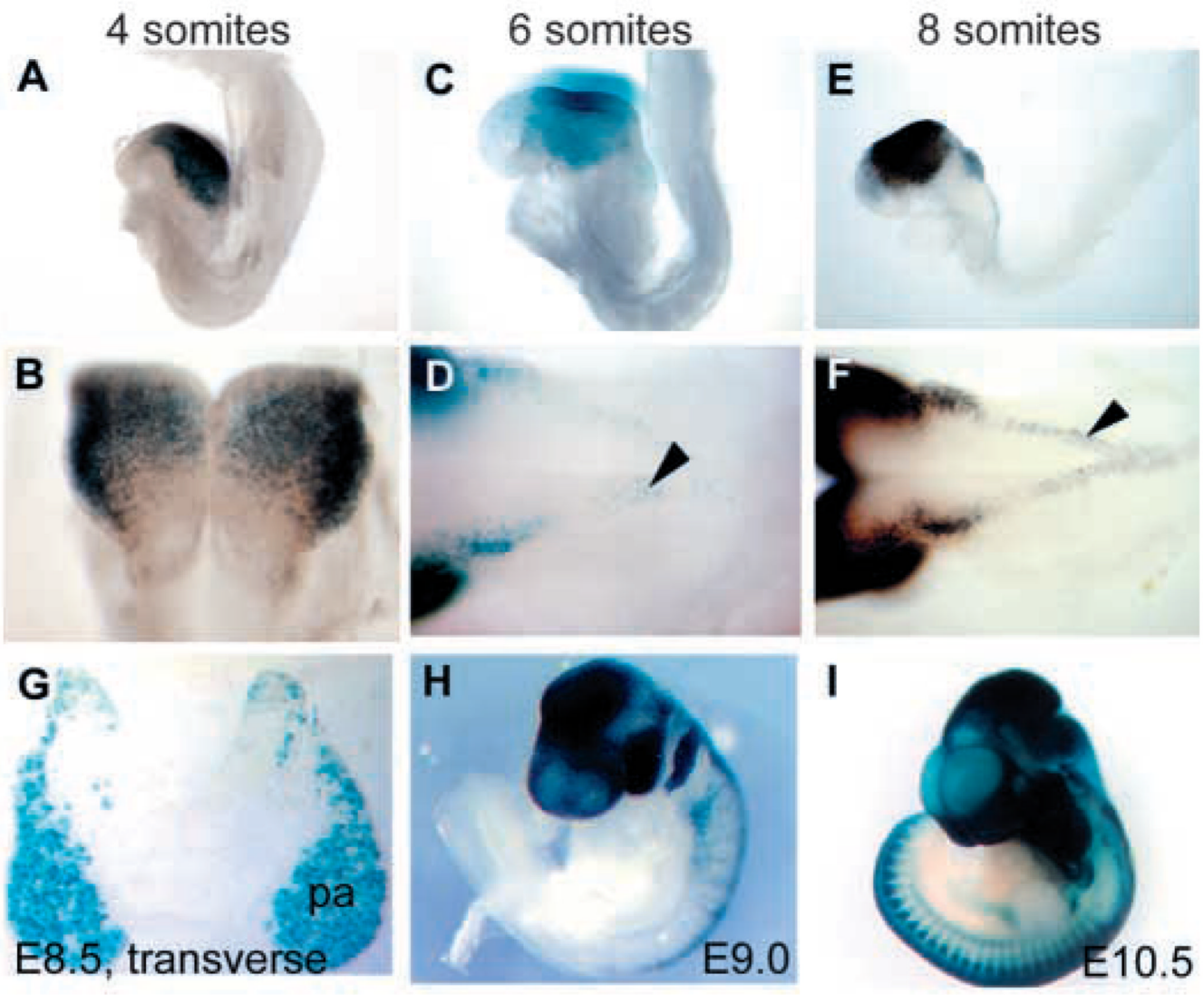

Fig. 1.

Wnt1-Cre recombination in the neural crest cells is marked by the expression of β-galactosidase in *Wnt1-Cre; R26R* embryos. (A,B) At 4 somites, *Wnt1-Cre* mediates loxP recombination in the forming NCCs of the hindbrain, but not the neural tube. (C,D) Multiple neural crest cells are positive for β-galactosidase activity in the neural tube at 6 somites. (E,F) NCCs are more plentiful at the eight-somite stage and are present at more caudal levels of the neural tube. Black arrowheads indicate the NCCs. B,D,F are dorsal, higher magnification views of embryos shown in A,C,E, respectively. Anterior is towards the top in B, towards the left in D,F. (G) A transverse section through the first pharyngeal arch (pa) of an embryo at similar stages to E,F. (H) E9.0 (15 somites) and (I) E10.5 embryos show caudal progression of *Wnt1-Cre* activity and increased NCC induction and migration.

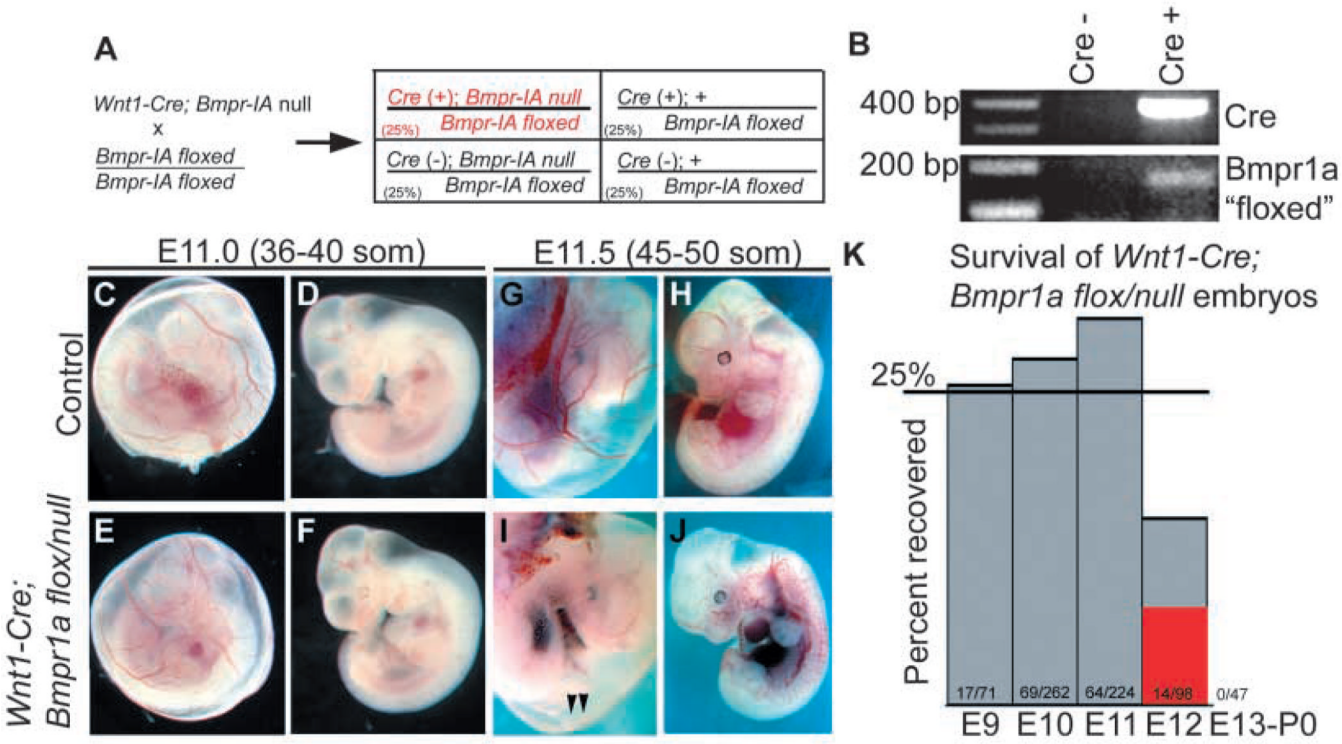

Fig. 2.

Ablation of *Bmpr1a* in neural crest cells. We have used the *Wnt1-Cre* transgene to ablate *Bmpr1a* activity in mouse NCCs. In the mating scheme outlined here (A), one quarter of the resulting embryos cannot transduce signals through BMPRIA in the neural crest. (B) PCR primers designed to detect recombined *Bmpr1a* alleles from genomic DNA show recombination from 15 s embryos only in the presence of Cre. (C–F) At E11.0, wild-type and *Wnt1-Cre; Bmpr1a*$^{flox/null}$ (mutant) embryos were morphologically indistinguishable. (G–J) Dissections at E11.5 showed an apparent lack of blood flow in mutant yolk sacs despite the presence of yolk sac blood vessels (I, arrows). Mutant embryos at E11.5 (J) show pooling of blood in peripheral vessels, heart, and liver. (K) Genotyping of dissected embryos reveals that *Wnt1-Cre; Bmpr1a*$^{flox/null}$ embryos are fully represented (Mendelian expectation is 25%) until E12.5. At E12.5, half of embryos recovered are in the process of resorption (red) and half are clearly necrotic. No mutants have been recovered after E12.5.

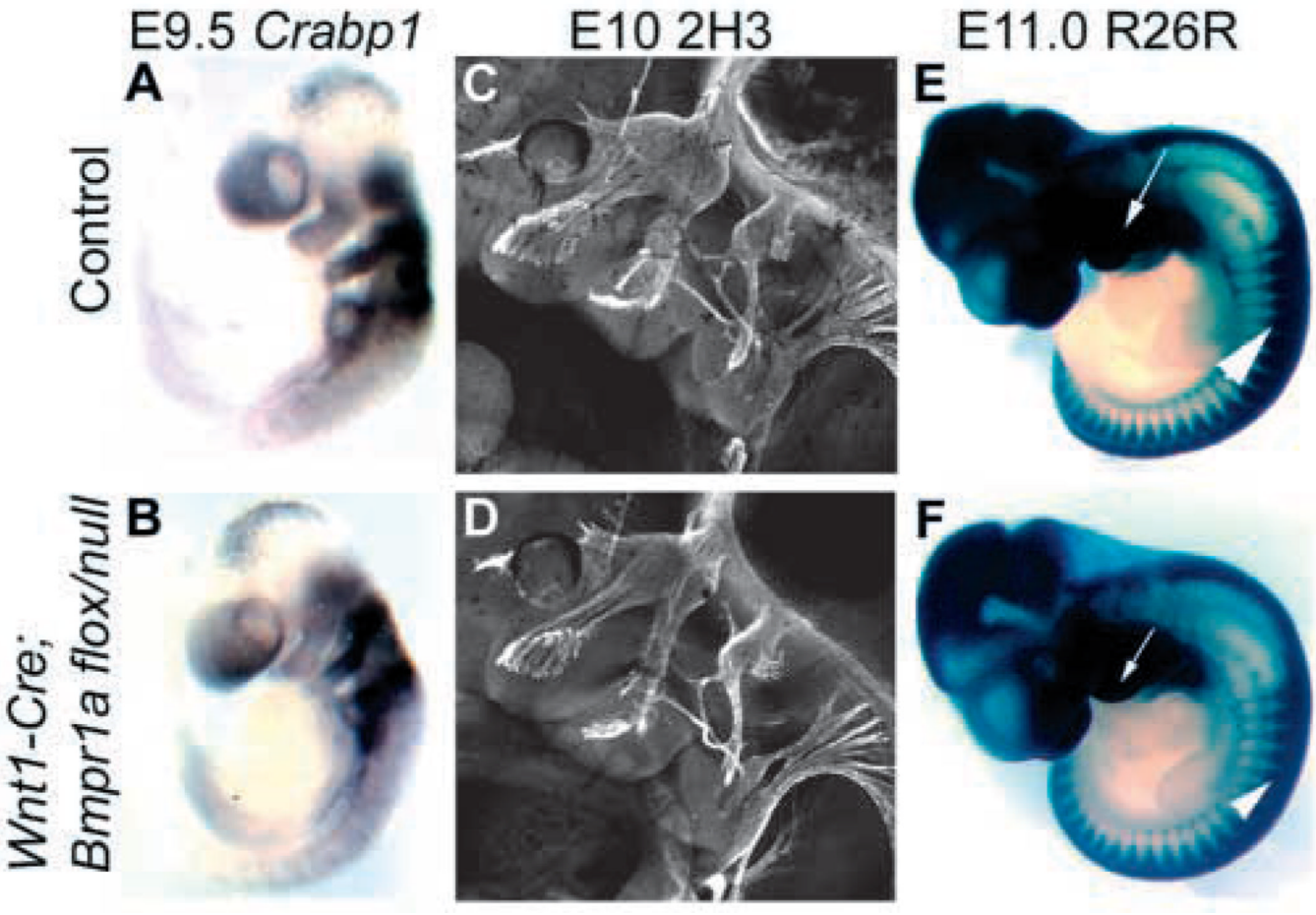

Fig. 3.

NCCs develop in BMPRIA NCC mutant embryos. (A,C,E) Wild-type, stage-matched control embryos for *Wnt1-Cre; Bmpr1a*$^{flox/null}$ mutants (B,D,F). (A,B) Expression of *Crabp1* and other neural crest markers showed normal NCC specification in mutants. (C,D) Immunostaining for neurofilaments with the 2H3 antibody showed proper differentiation of NCCs in mutants. (E,F) Mutant embryos expressing the *R26R* reporter, to label NCCs, show a normal distribution of NCCs and proper formation of many target tissues, including pharyngeal arches (arrows) and dorsal root ganglia (arrowheads).

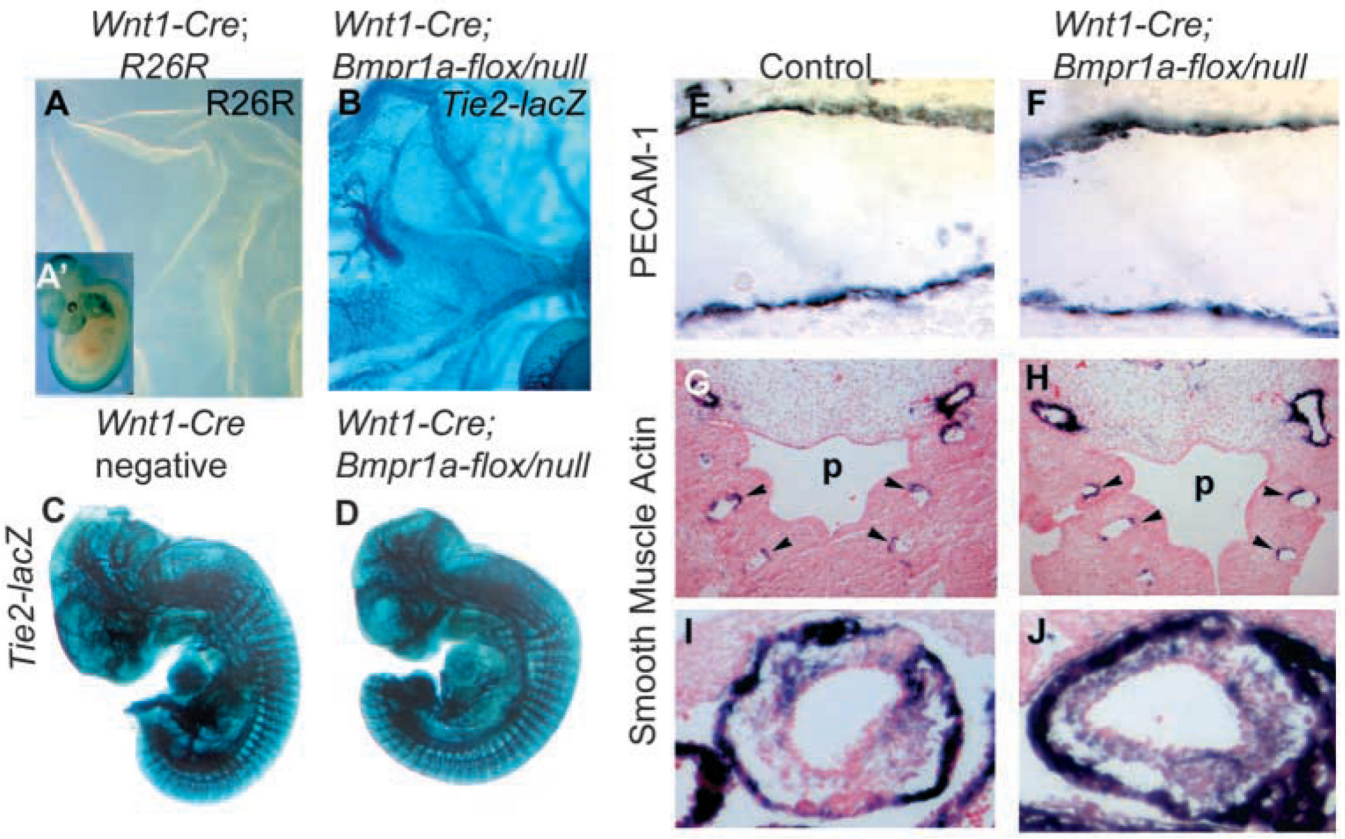

Fig. 4.

Normal vasculature in BMPRIA NCC mutants. (A) No *Wnt1-Cre* expressing cells were observed in yolk sacs (corresponding embryo in A′). Expression of a *Tie2-lacz* transgene marking endothelial cells showed no structural defect in mutant yolk sacs (B) or in mutant embryos (D) compared with controls (C). (E–J) Immunostaining for the endothelial marker, PECAM1 (E,F; sagittal sections through descending aorta) and for smooth muscle actin (G,H; coronal sections through pharyngeal arch arteries, highlighted by arrowheads; and I,J, coronal sections through outflow tract tissue) further confirm the lack of structural defects in peripheral vessels of mutants. p, pharynx. All paired images are shown at identical magnification.

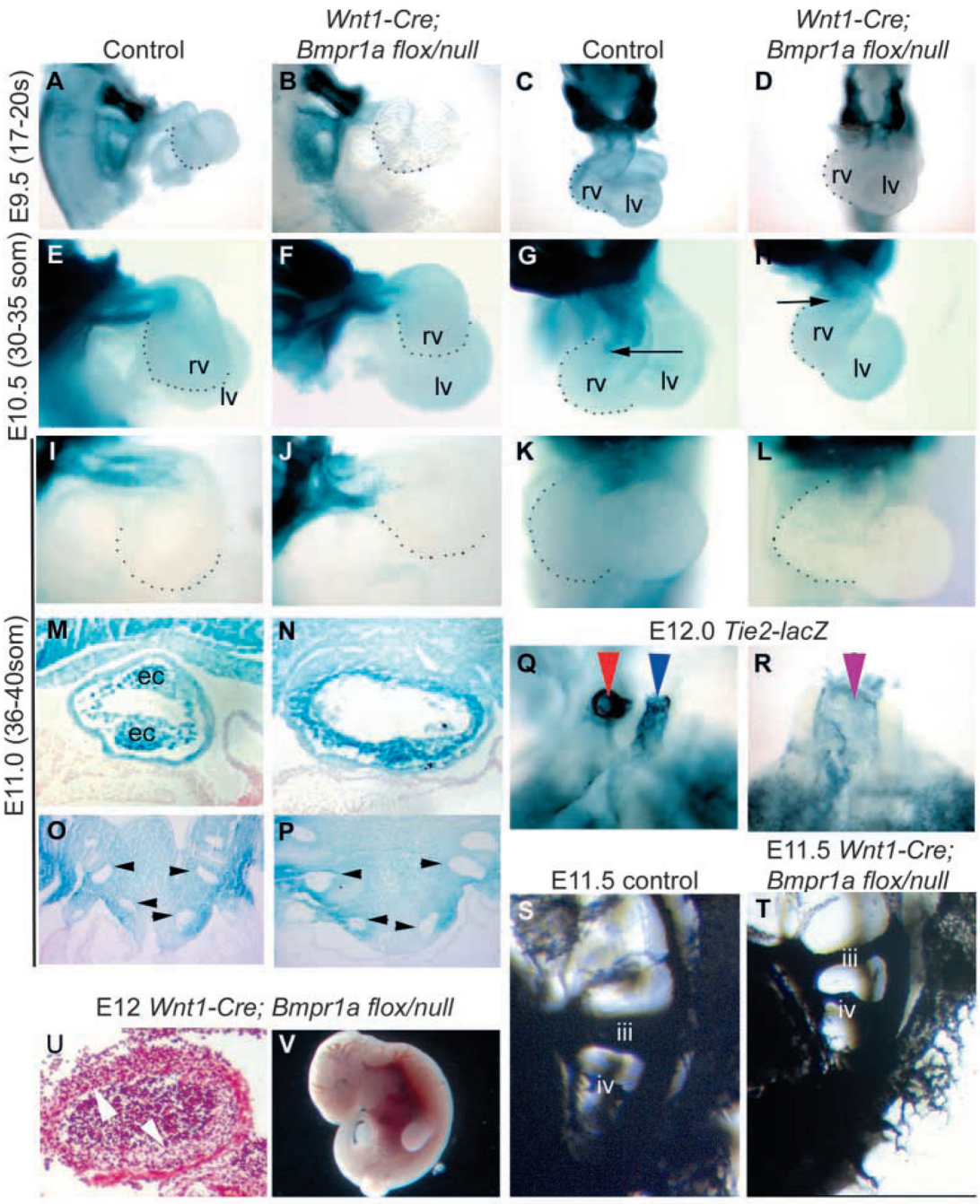

Fig. 5.

BMPRIA mutant embryos show cardiac outflow tract defects. (A–D) Dissections at E9.5 show mutant embryos (B,D) to have shortened outflow tract and future ventricular tissue (rv and lv indicate future right and left ventricle, respectively; broken lines indicate limit of the future right ventricle). These defects continue through E10.5 (E–H) and E11.5 (I–L) with reduced contributions of NCCs to outflow tract tissue clearly visible by E10.5 (H; black arrows highlight extent of NCC migration into outflow tract). (M–P) Frontal sections of E11.0 *Wnt1-Cre;Bmpr1a*$^{flox/null}$*; R26R* embryos (NCCs stained blue) show no occlusion of the outflow tract lumen (N) or aortic arch arteries (P, black arrowheads) but do reveal a reduction in endocardial cushion (ec) size compared with wild type (M). (Q,R) *Tie2-lacZ*

transgene expression marks endothelial cells, highlighting the lack of outflow tract septation in mutants at E12.0: red arrowhead indicates aorta, blue arrowhead indicates pulmonary artery, purple arrowhead indicates persistent (unseptated) truncus arteriosus. (S,T) Injection of ink into E11.5 ventricles shows dispersion through aortic sac to peripheral vasculature in both control and mutant embryos. Note the hypoplastic arch arteries evident in mutants (T; iii, third aortic arch artery; iv, fourth aortic arch artery). (U,V) Frontal section through a necrotic *Wnt1-Cre;Bmpr1a*$^{flox/null}$ embryo at E12 still reveals a blood filled, but unoccluded outflow tract. White arrows indicate lumenal edge. All paired images are shown at identical magnification.

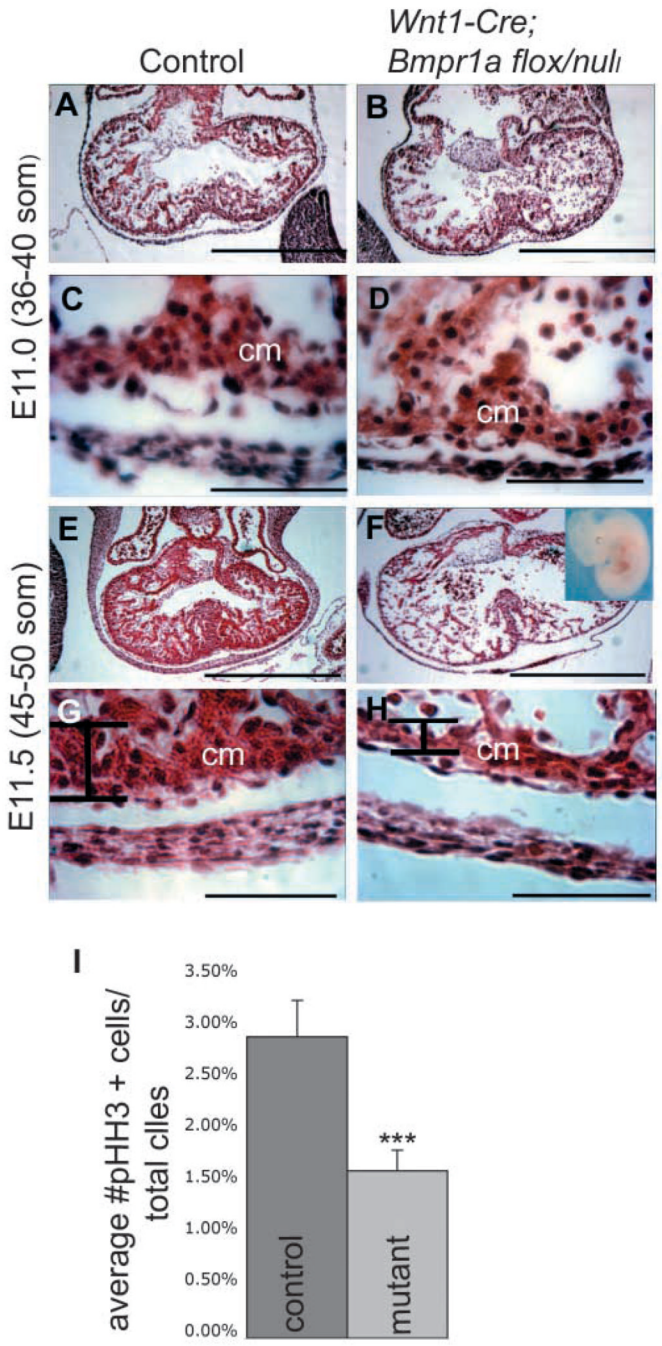

Fig. 6.

Embryos lacking BMPRIA in NCCs show defective ventricular myocardium by the 45–50 somite stage. Transverse sections of ventricles from embryos at E11.0 [36–40 somites (A–D)] and E11.5 [45–50 somites (E–H)]. The lower row shows higher magnification images from the sections immediately above. (B,D,F,H) Mutant *Wnt1-Cre;Bmpr1a*$^{flox/null}$ embryos; (A,C,E,G) wild-type (control) littermates. (A–D) Histological analysis of ventricular tissue revealed no mutant phenotype at E11.0, with mutant hearts (B,D) having similar degrees of compact myocardium (cm) as control hearts (A,C). (E–H) Control hearts at E11.5 (E,G) have robust compact myocardium as well as trabeculated myocardium occupying much of the ventricular chamber. Mutant hearts (F,H) have reduced compact and trabeculated

myocardium, observable prior to global necrosis (inset in F shows the embryo from which heart was taken; embryo appears healthy). (I) Proliferation rates were measured by counting cells stained for anti-phosphohistone H3 (pHH3+) as a percentage of the total at E10.5. A significant reduction (asterisks; $P<0.015$) was seen in mutant embryos. Scale bars: 250 μm for A,B,E,F; 32 μm for C,D,G,H.

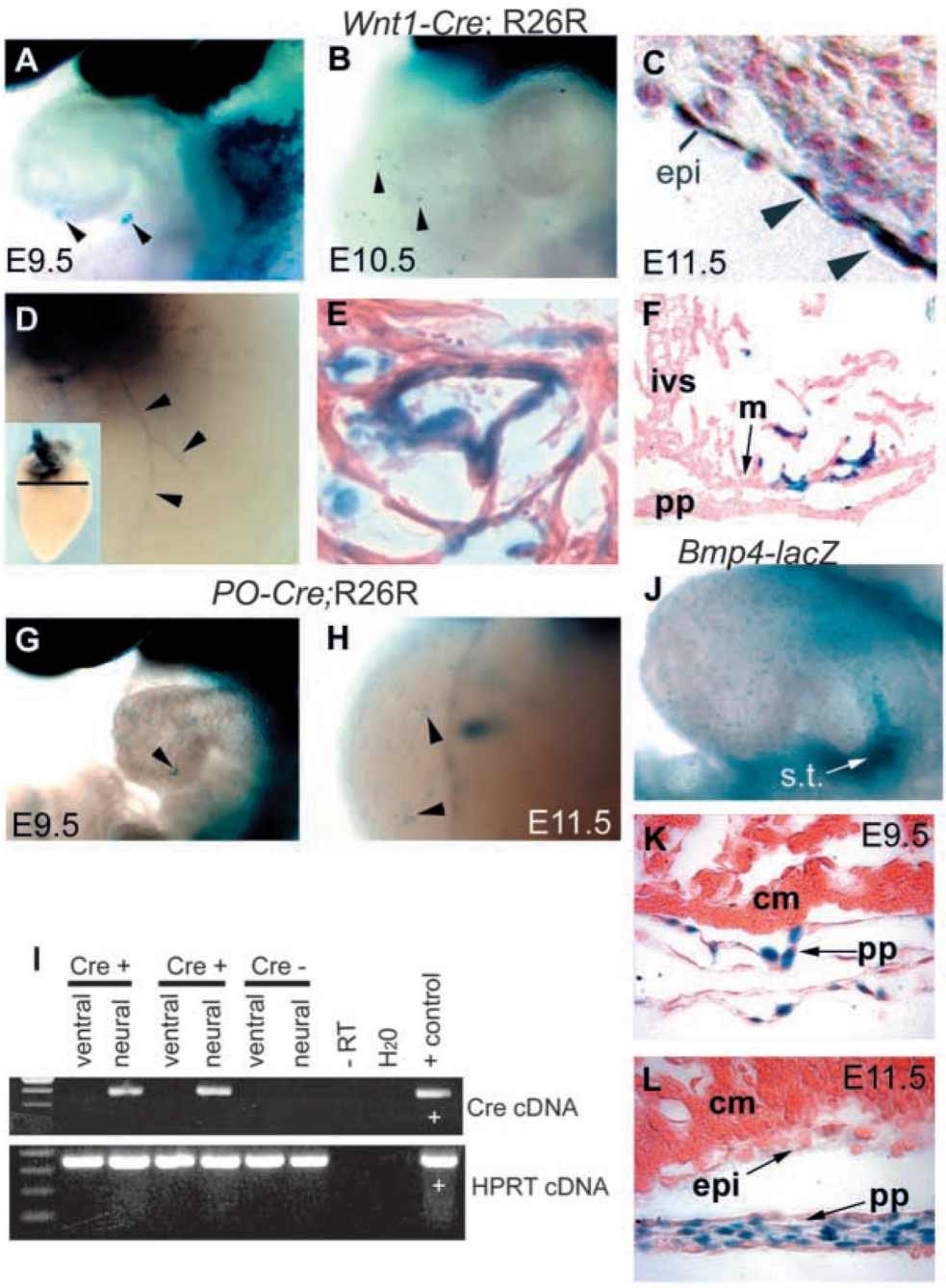

Fig. 7.

NCCs populate epicardium and ventricular myocardium. (A–C) *Wnt1-Cre*; *R26R* embryos showed blue β-galactosidase-positive cells (arrowheads) immediately caudal to the heart (abutting the septum transversum) and on the cardiac ventral surface, in the epicardium at E9.5 (A), E10.5 (B) and E11.5 (C). A transverse section of the heart (C,F) reveals stained cells in the epicardium (epi) and myocardium (m). ivs, interventricular septum; pp, parietal pericardium. (D,E) Neonatal *Wnt1-Cre; R26R* hearts show β-galactosidase-positive cells (arrowheads) contributing to the coronary vasculature, consistent with an epicardial lineage (inset shows entire heart shown in detail in D). (E) Sections through E17 hearts (relative plane of section indicated in D inset) indicate β-galactosidase-positive cells surrounding an

artery containing red blood cells. (G,H) Similar β-galactosidase-positive cells are seen in the epicardium of *PO-Cre; R26R* embryos. (I) RT-PCR analysis to assay for expression of *Wnt1-Cre* in ventral tissues. From each of two *Wnt1-Cre; R26R* embryos (Cre+) and one control *R26R* embryo (Cre−), RNA was isolated from tissues ventral to the dorsal aorta (ventral), including the heart and septum transversum, and the neural tube (neural). RNA was reverse-transcribed and subjected to PCR amplification of *Cre* or *Hprt* (positive control). HPRT was amplified from all samples except water (H_2O) or those prepared without reverse transcriptase (RT−). Cre was amplified only in the neural tube samples from Cre+ embryos. (J–L) *Bmp4-lacz* expression. Whole-mount embryos at E9.5 (J) and transverse sections at E9.5 (K) and E11.5 (L), showing high levels of *Bmp4* expression in the septum transversum (s.t.) and parietal pericardium (pp), but not epicardium. cm, compact ventricular myocardium.

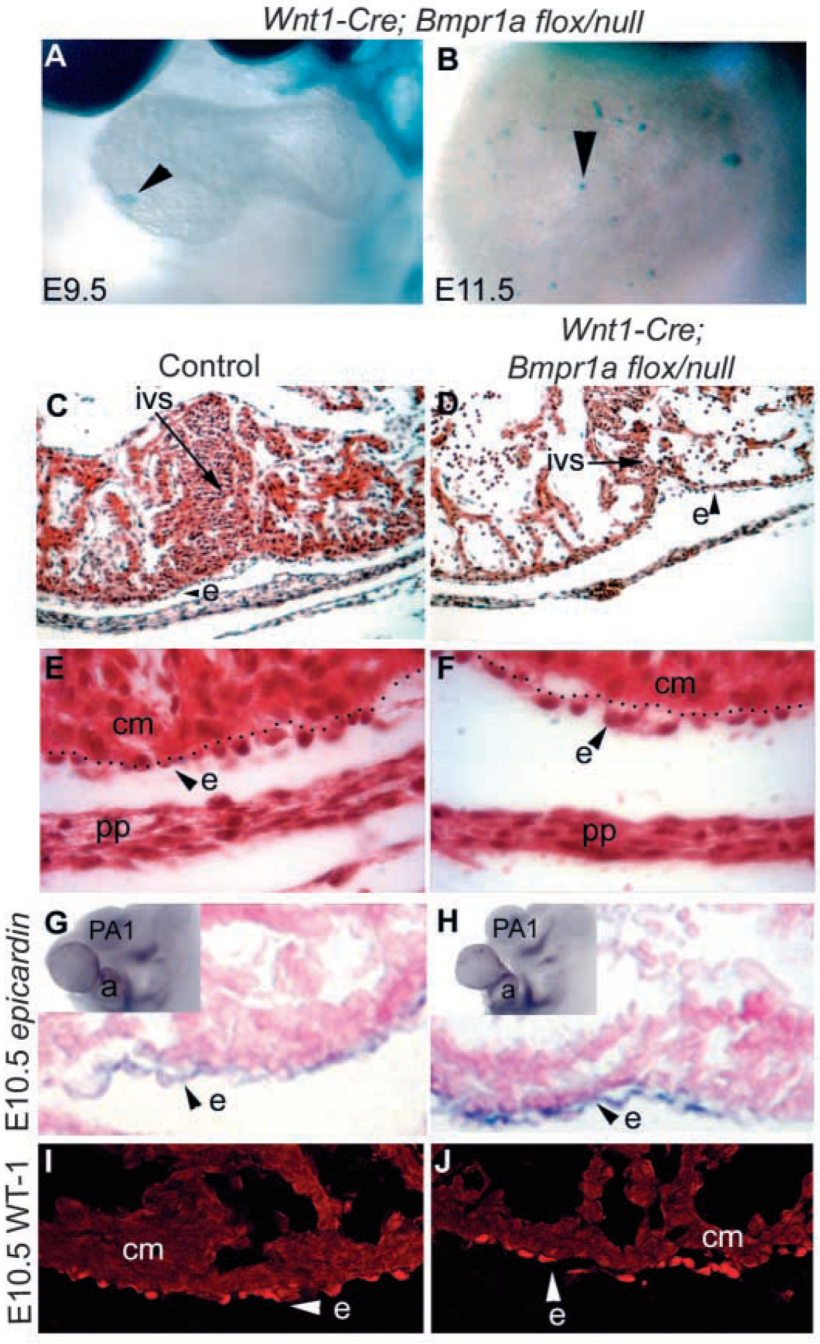

Fig. 8.

Epicardium appears normal in BMPRIA mutants. (A,B) NCCs appear in the same limited quantities in mutants as in control embryos at E9.5 (A) and E11.5 (B: compare to Fig. 7A,B). (C–F) Histological analysis (transverse sections) of the epicardium (e) at E11.5 shows no significant difference in the appearance of the epicardium of mutant tissue (D,F) which shows a clear ventricular myocardial phenotype (D, ivs: interventricular septum, pp: parietal pericardium). Dotted lines in E,F delineate the boundary between epicardium and compact ventricular myocardium. (G,H) In situ hybridization for *epicardin* also shows no defect in mutant epicardium (insets show that hybridization is specific to epicardial layer, pericardium was removed prior to in situ hybridization). (I,J) Immunohistochemistry for the

WT-1 protein shows no decrease in expression in the mutant in either the epicardium or the coelomic epithelial cells of the parietal pericardium (cm, compact ventricular myocardium). PA1, first pharyngeal arch; a, atrium; e, epicardium. All paired images are shown at identical magnification.

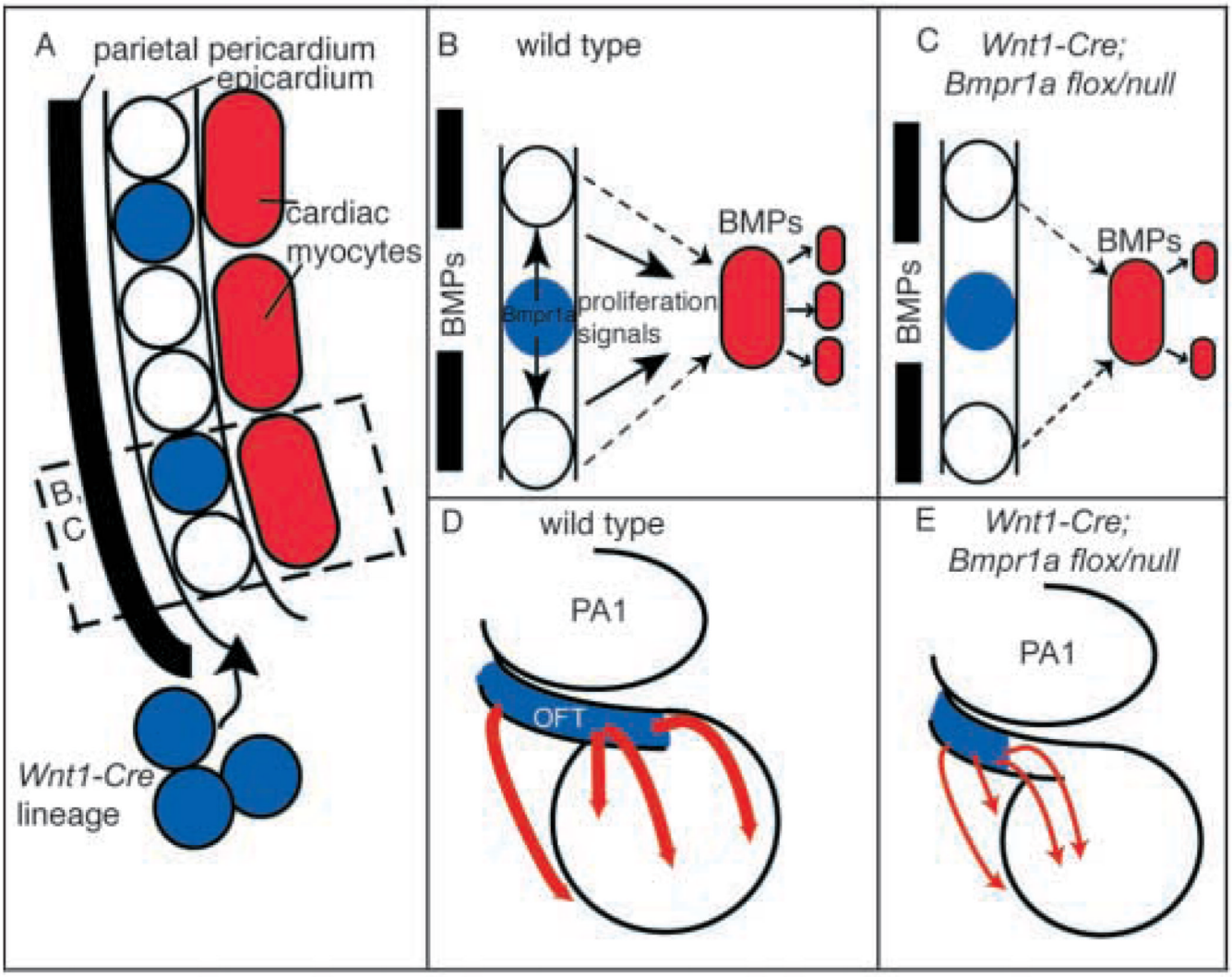

Fig. 9.

A model for the promotion of ventricular myocardium proliferation by BMP signaling in neural crest derivatives. (A) A limited population of cells in a *Wnt1-Cre* lineage (blue) migrates to the epicardium, located between the pericardial wall and ventricular myocardium. (B) Within the epicardium, these cells transduce signals through BMPRIA, resulting in the production of a proliferative signal, both *Bmpr1a* dependent (solid arrows) and *Bmpr1a* independent (broken arrows), for the underlying ventricular myocardium. BMP ligands for BMPRIA are expressed in both the pericardium and ventricular myocardium. In mutant embryos (C), although BMPs and cells of the *Wnt1-Cre* lineage are both still present, BMPRIA is not present in *Wnt1-Cre* positive cells. This results in decreased production of the unidentified trophic factor downstream of BMPRIA, leading to decreased myocardial proliferation. (D) An alternative explanation for the myocardial proliferation defects involves the cardiac neural crest of the outflow tract (OFT). These cells may produce a long range signal (red arrows) stimulating proliferation throughout the myocardium. (E) In mutant embryos, decreased migration of NCCs into the OFT results in decreased production of myocardial proliferation signals.

Table 1

Survival of *Wnt1-Cre; Bmpr1a*$^{flox/null}$ embryos

Age	*Cre negative; Bmpr1a*$^{+/flox}$	*Cre positive; Bmpr1a*$^{+/flox}$	*Cre negative; Bmpr1a*$^{null/flox}$	*Cre positive; Bmpr1a*$^{null/flox}$
E9	29	11	14	17 (24%)
E10	75	57	61	69 (26%)
E11	50	65	45	64 (29%)
E12	21	27	36	14* (14%)
E13	3	1	0	0† (0%)
E16	3	8	4	0† (0%)
P0	11	11	6	0 (0%)

*Seven out of 14 embryos recovered at E12 were in process of resorption; remaining embryos showed obvious signs of necrosis. Five more resorptions were genotyped as *Wnt1-Cre; Bmpr1a*$^{null/flox}$

†One resorption at E13 and five resorptions at E16 were recovered and genotyped as *Wnt1-Cre; Bmpr1a*$^{null/flox}$